JHEP

Published for SISSA by Springer

Received: May 12, 2015
Accepted: June 16, 2015
Published: July 9, 2015

Thermalization of Green functions and quasinormal modes

Justin R. David and Surbhi Khetrapal

Centre for High Energy Physics, Indian Institute of Science, C.V. Raman Avenue, Bangalore 560012, India

E-mail: justin@cts.iisc.ernet.in, surbhi@cts.iisc.ernet.in

Abstract: We develop a new method to study the thermalization of time dependent retarded Green function in conformal field theories holographically dual to thin shell AdS Vaidya space times. The method relies on using the information of all time derivatives of the Green function at the shell and then evolving it for later times. The time derivatives of the Green function at the shell is given in terms of a recursion formula. Using this method we obtain analytic results for short time thermalization of the Green function. We show that the late time behaviour of the Green function is determined by the first quasinormal mode. We then implement the method numerically. As applications of this method we study the thermalization of the retarded time dependent Green function corresponding to a minimally coupled scalar in the AdS_3 and AdS_5 thin Vaidya shells. We see that as expected the late time behaviour is determined by the first quasinormal mode. We apply the method to study the late time behaviour of the shear vector mode in AdS_5 Vaidya shell. At small momentum the corresponding time dependent Green function is expected to relax to equilibrium by the shear hydrodynamic mode. Using this we obtain the universal ratio of the shear viscosity to entropy density from a time dependent process.

Keywords: Gauge-gravity correspondence, Black Holes in String Theory, AdS-CFT Correspondence

ArXiv ePrint: 1504.04439

doi:10.1007/JHEP07(2015)041

JHEP07(2015)041

Contents

JHEP07(2015)041

1 Introduction

The question of how a highly excited state in a quantum system relaxes to equilibrium or how a quantum system relaxes when one of the parameters describing its Hamiltonian is quenched is of phenomenological interest. The relaxation of the state produced initially by high energy nuclear collisions from a highly excited state to quark-gluon plasma is an important question in the RHIC experiments [1]. Similarly the question of quenching of a quantum system can be studied experimentally in cold atoms where the coupling of an interacting system can be tuned to almost any value and in short time scales [2–5]. There have been various approaches, both analytical and numerical, developed to study these questions for a variety of quantum systems. When the question of thermalization is asked in quantum field theories which admit a holographic dual, the gauge/gravity correspondence links the question of approach to equilibrium in the field theory to the formation of a black hole in the bulk. See [6–10] for early studies pursuing this idea.

More recently motivated by success of the gauge/gravity duality to describe near equilibrium physics and hydrodynamic behaviour in strongly coupled field theories this question has received renewed attention which has resulted in more quantitative understanding [11–17]. In [13] the excited state in the quantum field theory was created by a translational invariant perturbation along the boundary of a minimally coupled scalar field. This perturbation lasted for a short duration of time. It was shown by solving the bulk equations that for a small amplitude of the perturbation, the metric outside the in-falling shell of matter is that of a black brane at the leading order. This result encouraged subsequent authors to model the collapse to a black hole by a homogenous in-falling shell of matter [18–24].

For definiteness we consider the thin shell model of collapse [21] given by the following metric

$$ds^2 = \frac{1}{z^2}\left[-(1-\theta(v)z^d)dv^2 - 2dzdv + d\mathbf{x}^2\right], \tag{1.1}$$
$$\theta(v) = \begin{cases} 0, & \text{for} \quad v < 0, \\ 1, & \text{for} \quad v \geq 0. \end{cases}$$

Here z refers to the radial co-ordinate, the boundary is at $z = 0$. $\mathbf{x} = x^1, \cdots x^{d-1}$ are the spatial co-ordinates at the boundary. The metric for $v < 0$ can be seen to be that of AdS_{d+1} using the following co-ordinate transformation

$$v = t - z. \tag{1.2}$$

While the metric for $v > 0$ reduces to that of the black brane in AdS_{d+1} under the co-ordinate transformation

$$dv = dt - \frac{dz}{1-z^d}. \tag{1.3}$$

From these co-ordinate transformations, we see that v coincides with time t at the boundary. We have chosen to work with units in which the radius of AdS_{d+1} is unity. The radius of the horizon is also unity. The Penrose diagram of the collapse is given in figure 1.

In [21] the study of how probes such as two point functions, Wilson loops and the entanglement entropy [25] thermalize in the thin shell Vaidya collapse was initiated. This study was mainly confined to the saddle point approximation of the probes. The behaviour of the probes were characterized in terms of their minimal geometric volume. In [23] the analysis was extended to study the two point function of operators dual to a minimally coupled massive scalar beyond the geodesic approximation for the case of the AdS_3 Vaidya shell. The retarded Green function $G_R(t_2, t_1; k)$ with time $t_1 < 0, t_2 > 0$, before and after the collapse of the shell was evaluated numerically. Translational invariance in the spatial direction of the collapsing shell (1.1) enabled the characterization of the Green function in the Fourier k space corresponding to the spatial directions. The analysis was numerical and it showed that the relaxation of the Green function is determined by the first quasinormal mode. In [24] the study of thermalizing Green functions was extended to fermions in the AdS_4 Vaidya shell. The analysis was again done numerically. Some analytic properties of the time dependent scalar Green functions was studied in [26].

JHEP07(2015)041

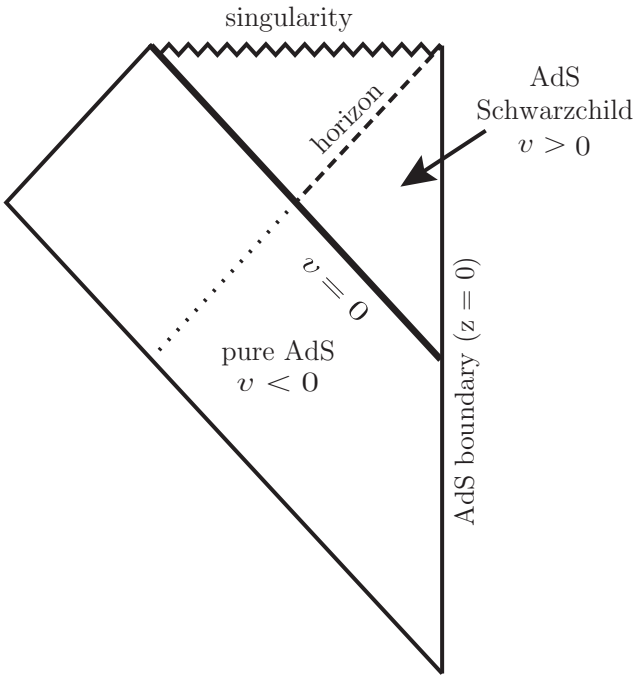

Figure 1. The Penrose diagram of collapse in AdS Vaidya.

In this paper we develop a new method to evaluate the retarded two point function $G_R(t_2, t_1; k)$ of an operator in the dual theory corresponding to the collapsing Vaidya AdS shell in the bulk. The method is general and can be implemented in arbitrary dimensions and for arbitrary types of fields in the bulk. The method relies on performing the matching of the wave functions corresponding to the dual fields before and after the shell term by term in the expansion of the radial co-ordinate z of (1.1). We will show that this enables the determination of all the time derivatives of G_R just after the collapse, $v = 0^+$ of the shell. It is then possible to evolve the Green function to an arbitrary future time t_2. On implementing this method we see that to obtain information of more and more higher derivatives of the Green function one needs to perform the matching of the wave functions of the bulk fields to higher powers in the radial coordinate z. This implies that one needs the information of the wave functions of these fields closer to the horizon to obtain long time behaviour of the Green function. It also implies that short time behaviour of the two point function after the collapse can be determined analytically from the near boundary information of the wave functions. Using the fact that the Green function at long time is determined by the near horizon behaviour of the wave functions we show that the relaxation of the Green function to equilibrium is determined by the first quasi-normal mode of the dual bulk field corresponding to the operator of interest in the black hole background.

We implement the method numerically and re-visit the case of the minimally coupled massive scalar in the AdS_3 Vaidya shell. We reproduce the results of [23]. We then study the case of the minimally coupled massless scalar in AdS_5 Vaidya shell. The Green function corresponding to this scalar is the retarded two point function of the spin 2 part of the

JHEP07(2015)041

stress tensor. We show that this Green function relaxes by the first quasi-normal mode which was determined numerically in [27]. We then study the vector fluctuations of the metric and obtain the Green function of the vector part of the stress tensor. For small momentum k, it is known [28] that this mode admits a hydrodynamic quasi-normal mode which obeys the dispersion relation given by

$$\omega = -i\frac{\eta}{Ts}k^2, \tag{1.4}$$

where η is the shear viscosity, s the entropy density and T the temperature of the fluid. We show the time dependent Green function corresponding to the vector fluctuations of the metric relaxes to equilibrium at small k by the hydrodynamic mode. Using this we determine the universal ratio of shear viscosity to entropy density from a time dependent process.

This paper is organized as follows. In the next section we detail the new method developed in this paper to evaluate the retarded Green function in collapsing AdS Vaidya thin shell backgrounds. We see that the method results in a recursion formula for the derivatives of the Green function just after the collapse of the shell. In section 3 we apply the method to obtain the Green function of the operator dual to the minimally coupled scalar in AdS_3 Vaidya shell. In section 4 we show that the long time behaviour of the Green function is determined by the first quasi-normal mode. This is first done for the case of AdS_3 Vaidya for which wave functions before and after the collapse of the shell are known exactly. Then the argument is extended in general for any Green function. In section 5 we turn to the case of AdS_5 Vaidya. We first study the thermalization of the shear correlator of the stress tensor by solving the minimally coupled scalar in AdS_5 Vaidya. We then examine the vector perturbations of the metric to evaluate the two point function of the spin-1 part of the stress tensor and show that it relaxes at small momentum by the shear hydrodynamic mode. Section 6 contains the conclusions. Appendices A to D deal with technical details required for the analysis in the paper.

2 Recursion method for time dependent Green functions

In this section we will outline the general method to obtain the retarded Green function in the thin shell Vaidya AdS geometry. The method is general, and can be applied to any field in the AdS_{d+1} Vaidya geometry given in (1.1). For definiteness let us focus on the minimally coupled scalar of mass m. The differential equation obeyed by ϕ is given by

$$h(v,z)\partial_z^2\phi + \left(\frac{1}{z}\partial_v\phi - 2\partial_v\partial_z\phi\right) + \left(\partial_z h - \frac{h(v,z)}{z}\right)\partial_z\phi - \left(\frac{m^2}{z^2} + k^2\right)\phi = 0, \tag{2.1}$$

where

$$h(v,z) = 1 - \theta(v)z^d, \tag{2.2}$$

and k is the Fourier conjugate of direction x^{d-1}.

The solution $\phi^{\rm AdS}$ in the region $v < 0$ corresponding to before the formation of the black hole admits a closed form in terms of Bessel functions. The analytical solution will

JHEP07(2015)041

be explicitly discussed in the examples we will consider subsequently. The solution has the form

$$\phi^{\rm AdS}(v,k,z;t_1) = z^{\Delta_+} J(v-t_1,k,z), \tag{2.3}$$

where $\Delta_+ > \Delta_-$ are the two solutions of the equation

$$\Delta(\Delta - d) = m^2. \tag{2.4}$$

The solution we choose satisfies the boundary condition

$$\phi^{\rm AdS}(v,k,z;t_1) \xrightarrow{z\to 0} z^{\Delta_-}\delta(v-t_1) + \ldots, \tag{2.5}$$

with $t_1 < 0$. This is necessary to obtain the retarded Green function. In (2.3) note that due to time translational symmetry for $v < 0$, the wave function just depends on the combination $v - t_1$. In the black hole region $v > 0$, the bulk equations of motion usually do not admit a closed form solution. But the solution in the frequency ω and momentum k domain can be constructed in terms of a Frobenius series around the boundary $z = 0$. Then the most general solution in the time domain $v > 0$ can be obtained by taking Fourier transform of the two independent solutions obtained by the Frobenius method with respect to the frequency, ω. We write this as

$$\phi^{BH}(v,k,z) = \int_{-\infty}^{\infty} d\omega e^{-i\omega v} \sum_{n=0}^{\infty} \left[z^{\Delta_+} C(\omega,k) A_n(\omega,k) z^n + z^{\Delta_-} D(\omega,k) B_n(\omega,k) z^n \right]. \tag{2.6}$$

Note that here we have assumed that the roots of the indicial equation of (2.1), Δ_+, Δ_- do not differ from each other by an integer. The discussion can be carried out for the case when the roots differ by an integer but as we will see that we will only need the less singular solution which falls of as z^{Δ_+} to construct the retarded Green function. $C(\omega,k)$ and $D(\omega,k)$ in (2.6) are functions which must be determined by continuity at $v = 0$. Note that the coefficients of the differential equation (2.1) are discontinuous, but the discontinuity is finite across $v = 0$, therefore the solution ϕ must be continuous at $v = 0$. Thus we have

$$\phi^{\rm AdS}(v=0,k,z;t_1) = \phi^{BH}(v=0,k,z). \tag{2.7}$$

We impose continuity by equating each term of the power series in z about the boundary. Thus we expand both sides of (2.7) in powers of z and obtain the equation

$$z^{\Delta_+} \sum_{n=0}^{\infty} \tilde{J}_n z^n + z^{\Delta_-}\delta(-t_1) = \int_{-\infty}^{\infty} d\omega \sum_{n=0}^{\infty} \left(z^{\Delta_+} C(\omega) A_n(\omega) z^n + z^{\Delta_-} D(\omega) B_n(\omega) z^n \right). \tag{2.8}$$

We have suppressed the dependence of $\tilde{J}_n$ on t_1, k and the dependence of $C(\omega), A_n$, $D(\omega), B_n$ on k to un-clutter the equations. Equating the coefficients of z^n in the terms proportional to z^{Δ_+} we obtain

$$\tilde{J}_n = \int_{-\infty}^{\infty} d\omega\, C(\omega) A_n(\omega). \tag{2.9}$$

JHEP07(2015)041

From the examples considered in the paper, it is seen that $A_n(\omega)$ is an n-th order polynomial in ω.[1] Therefore we write A_n as

$$A_n = \sum_{j=0}^{n} a_n^j \omega^j. \tag{2.10}$$

Substituting this expansion in (2.9) we obtain

$$\tilde{J}_n = \sum_{j=0}^{n} a_n^j \int_{-\infty}^{\infty} d\omega\, C(\omega)\omega^j. \tag{2.11}$$

Let us define the j-th moment of $C(\omega)$ as,

$$M_j = \int_{-\infty}^{\infty} d\omega\, C(\omega)\omega^j. \tag{2.12}$$

Substituting this in equation (2.11), we can rewrite it as,

$$\tilde{J}_n = \sum_{j=0}^{n} a_n^j M_j. \tag{2.13}$$

This equation can be inverted to obtain the moments, M_j, which contain information about $C(\omega)$. Note that a_n^j are known from Frobenius series solution ϕ^{BH}. Therefore we obtain

$$M_n = \frac{1}{a_n^n}\left(\tilde{J}_n - \sum_{j=0}^{n-1} a_n^j M_j\right); \quad n > 0, \tag{2.14}$$

$$M_0 = \frac{\tilde{J}_0}{a_0^0}. \tag{2.15}$$

Knowledge of all the moments M_j is sufficient to construct the retarded Green function. To see this consider the near boundary behaviour of the field ϕ. From equations (2.5), (2.6) and (2.8), the near boundary behaviour of the field for $v > 0$ is given by

$$\phi^{BH}(v, t_1, k) = \int_{-\infty}^{\infty} d\omega e^{-i\omega v} C(\omega) z^{\Delta_+} A_0 + \cdots + O(z^{\Delta_-}). \tag{2.16}$$

Together with the boundary condition (2.5), the AdS/CFT recipe for the retarded Green function [29] states that it is given by

$$G_R(v) = \int_{-\infty}^{\infty} d\omega e^{-i\omega v} C(\omega). \tag{2.17}$$

Here we have ignored overall proportionality constants in the Green function to simplify the discussion. Expanding the exponential as Taylor series, and using the definition of the moments of $C(\omega)$ we obtain

$$G_R(v) = \sum_{n=0}^{\infty} \frac{(-iv)^n M_n}{n!}. \tag{2.18}$$

[1] This can be seen using the recursion formula obtained during the construction of the Frobenius series solution of (2.1).

JHEP07(2015)041

Thus the knowledge of all the moments of $C(\omega)$ is sufficient to construct the Green function. Note that knowledge of $D(\omega)$ in (2.6) is not necessary. We call this the recursion method to obtain the Green function since each term in (2.18) is given recursively from the knowledge of the lower moments using (2.14). It allows for the construction of the the Green function as a power series in time for $v > 0$. The information of t_1 is present in $\tilde{J}_n$ and all terms depend on momentum k. There is another way to view this construction of the retarded Green function. Note that the j-th moment of $C(\omega)$ is essentially the j-th derivative of the Green function, evaluated at $v = 0^+$,

$$\frac{\partial^j G_R}{\partial v^j}\Big|_{v=0^+} = \int_{-\infty}^{\infty} d\omega\, (-i\omega)^j C(\omega) = (-i)^j M_j. \tag{2.19}$$

Thus this method determines the Green function for $v > 0$ from the knowledge of all its time derivatives at $v = 0^+$.

We now make some general properties of this method of determining the retarded Green function. Since the method relies on construction of ϕ^{BH} using the Frobenius series we can apply it in general to all black hole backgrounds even if closed form solutions do not exist. The method can be applied even if the background is only known in terms of a power series in z about the boundary for example in finite temperature versions of RG flow solutions [30]. Note that for short time development of the Green function for $v > 0$, knowledge of only a few moments is needed. This implies from (2.18) and (2.14) we need the knowledge of wave functions before and after $v = 0$ close to the boundary. That is we need the knowledge of the wave functions to a few powers of z. Thus short time development of the Green function can be written down analytically by obtaining a few moments. However for the long time behaviour of the Green function we need to know a large number of moments. Again from (2.14), this implies we need the information of the wave function for large powers of z which in turn implies that we need the behaviour close to the horizon. This fits with the general intuition that long time behaviour is controlled by the behaviour near the horizon. It is this property which will enable us to prove that the long time behaviour of the Green function is determined by the quasinormal mode in section 4. Finally, it will turn out that even moments are real and odd moments are purely imaginary. This is because the coefficients a_n^j for odd j are imaginary. This is easily seen due to the fact that each power of ω comes with a factor of i. Then from (2.14) it is easy to see that even moments are real and odd moments are purely imaginary. This then ensures that the Green function given by (2.18) is real.

3 Thermalization in AdS_3 Vaidya

In this section we will implement the method developed in section 2 for the case of thin shell Vaidya metric in AdS_3. We study the thermalization of the retarded Green function of the operator corresponding to the minimally coupled scalar of mass m. We will show that using our method we reproduce the results of [23]. We also determine a few low moments analytically to obtain the short time behaviour of the Green function. A simplification that occurs for the case of the AdS_3 is that the solutions of the minimally coupled scalar in the

JHEP07(2015)041

BTZ black hole are known in closed form in terms of hypergeometric functions [31]. These solutions will provide the initial starting point in our argument to demonstrate that the long time behaviour of the Green function is determined by the lowest quasi-normal mode.

The thin-shell AdS-Vaidya metric, in 3 dimensions is given by

$$\begin{aligned} ds^2 &= \frac{1}{z^2}\left[-h(z,v)dv^2 - 2dvdz + d\phi^2\right], \\ h(z,v) &= 1-\theta(v)z^2. \end{aligned} \tag{3.1}$$

The co-ordinate ϕ parametrizes the spatial direction of the field theory and we assume that it is not compact. The scalar field equation in this metric is given by

$$h\partial_z^2\Phi + \left(\frac{1}{z}\partial_v\Phi - 2\partial_v\partial_z\Phi\right) + \left(\partial_z h - \frac{h}{z}\right)\partial_z\Phi - \left(\frac{m^2}{z^2}+k^2\right)\Phi = 0. \tag{3.2}$$

3.1 Scalar wave functions in AdS_3 Vaidya shell

We solve the minimally coupled massive scalar equation given in (3.2). We discuss the solutions before and after the collapse of the shell below.

Solution for $v<0$. The solution for the scalar field for $v<0$ is given by [23]

$$\begin{aligned} &\Phi^{\rm AdS}(v-t_1,k,z) \\ &= C\frac{\theta(v-t_1)z^{\Delta_+}}{[(v-t_1)^2+2(v-t_1)z]^{\frac{2\nu+1}{4}}}|k|^{\nu+\frac{1}{2}}J_{-\nu-\frac{1}{2}}\left(|k|\sqrt{(v-t_1)^2+2(v-t_1)z}\right), \end{aligned} \tag{3.3}$$

$$C = \frac{2^{\frac{1}{2}-\nu}\sqrt{\pi}}{\Gamma(\nu)}. \tag{3.4}$$

Note that this solution is written down in mixed Fourier space (t,k). Here $\Delta_\pm$ are solutions to the quadratic equation $\Delta(\Delta-2)=m^2$ and are given by

$$\Delta_\pm = 1\pm\nu, \quad \nu=\sqrt{1+m^2}. \tag{3.5}$$

This solution satisfies the required boundary condition discussed in (2.5) which is required to evaluate the retarded Green function,

$$\Phi^{\rm AdS}(v-t_1,k,z) = \delta(v-t_1)z^{\Delta_-}+\ldots. \tag{3.6}$$

To show this we first take the the limit $z\to 0$ in (3.3) keeping $v-t_1\neq 0$. We see that there is no term proportional to z^{Δ_-}. Now we take $v\to t_1$, the wave function then reduces to

$$\Phi^{\rm AdS}(k,v,z)_{z\to 0} = \frac{\theta(v-t_1)2\sqrt{\pi}}{\Gamma(-\nu+\frac{1}{2})\Gamma(\nu)}\frac{z^{\Delta_+}}{[(v-t_1)^2+2(v-t_1)z]^{\nu+\frac{1}{2}}}. \tag{3.7}$$

This solution certainly diverges in the limit $v\to t_1$. All what one needs to show is that the expression in (3.7) is a representation of the delta function times z^{Δ_-}. To demonstrate this we perform the integral over v as follows

$$\begin{aligned} \int_{-\infty}^{\infty} dv\,\Phi^{\rm AdS}(k,v,z)_{z\to 0} &= \frac{2\sqrt{\pi}}{\Gamma(-\nu+\frac{1}{2})\Gamma(\nu)}z^{\Delta_-}\int_{-\infty}^{\infty}\frac{dv}{z}\theta(v-t_1)\frac{1}{[(\frac{v-t_1}{z}+1)^2-1]^{\nu+\frac{1}{2}}} \\ &= z^{\Delta_-}. \end{aligned} \tag{3.8}$$

Therefore we conclude that the solution in (3.3) satisfies the required boundary condition given in (3.6).

JHEP07(2015)041

Solution for $v > 0$. The strategy to obtain a closed form solution for $v > 0$ is as follows. Note that under the transformation

$$t = v - \frac{1}{2}\ln\left(\frac{1-z}{1+z}\right), \tag{3.9}$$

the metric given in (3.1) for $v > 0$ reduces to that of the BTZ black hole in Poincaré coordinates. This is given by

$$ds^2 = \frac{1}{z^2}\left(-(1-z^2)dt^2 + \frac{dz^2}{1-z^2} + d\phi^2\right). \tag{3.10}$$

Now the solutions to the minimally coupled scalar in the BTZ black hole is known [31]. The two independent solutions are given by

$$\begin{aligned}\Phi^{(1)}_{\omega,k}(z,t,\phi) &= e^{-i\omega t+ik\phi}(1-z^2)^{-\frac{i\omega}{2}}z^{\Delta_-} \\ &\quad\times F\left(\frac{1}{2}(\Delta_- - i(\omega-k)), \frac{1}{2}(\Delta_- - i(\omega+k)), 1-i\omega, 1-z^2\right), \\ \Phi^{(2)}_{\omega,k}(z,t,\phi) &= e^{-i\omega t+ik\phi}(1-z^2)^{\frac{i\omega}{2}}z^{\Delta_-} \\ &\quad\times F\left(\frac{1}{2}(\Delta_- + i(\omega+k)), \frac{1}{2}(\Delta_- + i(\omega-k)), 1+i\omega, 1-z^2\right).\end{aligned} \tag{3.11}$$

Note that these two independent solutions reduce to the ingoing and outgoing Fourier modes at the horizon. We can now obtain the solution in the coordinates (z, v, ϕ) by performing the substitution given in (3.9). This leads to the following independent solutions for the Vaidya metric in the region $v > 0$,

$$\begin{aligned}\Phi^{(1)}_{\omega,k}(z,v,\phi) &= e^{-i\omega v+ik\phi}(1+z)^{i\omega}z^{\Delta_-} \\ &\quad\times F\left(\frac{1}{2}(\Delta_- - i(\omega-k)), \frac{1}{2}(\Delta_- - i(\omega+k)), 1-i\omega, 1-z^2\right), \\ \Phi^{(2)}_{\omega,k}(z,v,\phi) &= e^{-i\omega v+ik\phi}(1-z)^{i\omega}z^{\Delta_-} \\ &\quad\times F\left(\frac{1}{2}(\Delta_- + i(\omega+k)), \frac{1}{2}(\Delta_- + i(\omega-k)), 1+i\omega, 1-z^2\right).\end{aligned} \tag{3.12}$$

Now the above solutions admit an expansion around the horizon $z = 1$, however we have seen in section 2, to obtain the Green function we need an expansion around the boundary $z = 0$. This can be achieved by using the transformation properties of the hypergeometric functions. We have performed the required transformation in appendix A. This results in the following independent solutions,

$$\begin{aligned}\Phi^{\mathrm{BTZ}(+)}_{\omega,k}(z,v,\phi) &= e^{-i\omega v+ik\phi}(1+z)^{i\omega}z^{\Delta_-}\times \\ &\quad F\left(\frac{1}{2}(\Delta_- - i(\omega-k)), \frac{1}{2}(\Delta_- - i(\omega+k)), \Delta_-, z^2\right), \\ \Phi^{\mathrm{BTZ}(-)}_{\omega,k}(z,v,\phi) &= e^{-i\omega v+ik\phi}(1+z)^{i\omega}z^{\Delta_+}\times \\ &\quad F\left(\frac{1}{2}(\Delta_+ - i(\omega+k)), \frac{1}{2}(\Delta_+ - i(\omega-k)), \Delta_+, z^2\right).\end{aligned} \tag{3.13}$$

JHEP07(2015)041

It can be explicitly verified that the above solutions satisfy the equations of motion given in (3.2) for $v > 0$. The partial Fourier transform of this solution with respect to ω is given by

$$\begin{aligned}
&\Phi^{\rm BTZ}(k,v,z) \qquad (3.14)\\
&= z^{\Delta_-}\int_{-\infty}^{\infty} d\omega\, e^{-i\omega v}\, C_1(\omega)(1+z)^{-i\omega} F\left(\frac{1}{2}(\Delta_- - i(\omega-k)), \frac{1}{2}(\Delta_- - i(\omega+k)), \Delta_-, z^2\right)\\
&+ z^{\Delta_+}\int_{-\infty}^{\infty} d\omega\, e^{-i\omega v}\, C_2(\omega)(1+z)^{-i\omega} F\left(\frac{1}{2}(\Delta_+ - i(\omega+k)), \frac{1}{2}(\Delta_+ - i(\omega-k)), \Delta_+, z^2\right).
\end{aligned}$$

The above solution admits an expansion around the boundary $z = 0$. Therefore we have written the solution in the black hole region in the required form given in (2.6). Note that in the case of the BTZ black hole, the Frobenius expansion around the boundary can be written in closed form.

3.2 Matching at $v = 0$ and Green function

We follow the general procedure discussed in section 2 to construct the time dependent Green function. To do this we first obtain the moments of the function $C_2(\omega)$ by matching the wave function $\Phi^{\rm AdS}(v,k,z)$ in (3.3) and $\Phi^{\rm BTZ}(v,k,z)$ in (3.13) at $v = 0$. The moments of $C_2(\omega)$ are determined by comparing powers of z in the terms proportional to z^{Δ_+}. We will demonstrate this procedure explicitly and obtain moments up to the second order. We expand the l.h.s. of (3.3) and the z^{Δ_+} coefficient of (3.13) to quadratic order in z to obtain the following equation

$$\begin{aligned}
&C\theta(-t_1)\left(\frac{|k|}{|t_1|}\right)^{\nu+\frac{1}{2}}\left(1+\left(\frac{\nu}{2}+\frac{1}{4}\right)\left(\frac{2z}{t}\right)+\frac{1}{2!}\left(\frac{\nu}{2}+\frac{1}{4}\right)\left(\frac{\nu}{2}+\frac{5}{4}\right)\left(\frac{2z}{t}\right)^2\ldots\right)\times\\
&\left(J_{-\nu-\frac{1}{2}}(|k||t_1|)+z\frac{dJ_{-\nu-\frac{1}{2}}\left(|k|\sqrt{t_1^2-2t_1z}\right)}{dz}\Big|_{z=0}+\frac{z^2}{2}\frac{d^2J_{-\nu-\frac{1}{2}}\left(|k|\sqrt{t_1^2-2t_1z}\right)}{dz^2}\Big|_{z=0}+\ldots\right)\\
&=\int_{-\infty}^{\infty} d\omega C_2(\omega)\left(1-i\omega z+i\omega(i\omega+1)\frac{z^2}{2}+\ldots\right)\times\\
&\quad\times\left(1+\frac{\frac{1}{2}(1+\nu-i(\omega+k))\frac{1}{2}(1+\nu-i(\omega-k))}{1+\nu}z^2+\ldots\right)\\
&=\int_{-\infty}^{\infty} d\omega C_2(\omega)\left(1-i\omega z+\left(\frac{1+\nu}{4}-\frac{\omega^2}{2}-\frac{\omega^2-k^2}{4(1+\nu)}\right)z^2+\ldots\right). \qquad (3.15)
\end{aligned}$$

Comparing the terms we can read out the moments to quadratic order. These are given by

$$\begin{aligned}
M_0 &= \int_{-\infty}^{\infty} d\omega\, C_2(\omega) = NJ_{-\nu-\frac{1}{2}}(|k||t_1|), \qquad (3.16)\\
M_1 &= \int_{-\infty}^{\infty} d\omega\, wC_2(\omega) = -iNkJ_{-\nu-\frac{3}{2}}(|k||t_1|),\\
M_2 &= \int_{-\infty}^{\infty} d\omega\, w^2C_2(\omega) = N\Bigg[\left(\frac{(1+\nu)^2}{3+2\nu}+k^2-\frac{2(1+\nu)(1+2\nu)}{t_1^2}\right)J_{-\nu-\frac{1}{2}}(|k||t_1|)\\
&\qquad -\frac{2k(1+\nu)}{t_1}J_{-\nu+\frac{1}{2}}(|k||t_1|)\Bigg],
\end{aligned}$$

JHEP07(2015)041

here, $N \equiv C\theta(-t_1)\left(\frac{|k|}{|t_1|}\right)^{\nu+\frac{1}{2}}$. As discussed in section 2, see equation (2.18), the retarded Green function is given by[2]

$$G(v) = M_0 + ivM_1 - \frac{1}{2!}v^2 M_2 + \cdots . \tag{3.17}$$

Thus it is clear that the short time expansions of the Green function can be easily obtained.

It is interesting to take the $k = 0$ limit of the moments and construct the short time expansion of the Green function. In this limit the Bessel function reduces to a rational function and the first few moments are given by

$$\begin{aligned} M_0 &= \frac{C}{t_1^{2\nu+1}} \frac{2^{\nu+\frac{1}{2}}}{\Gamma(-\nu+\frac{1}{2})}, \\ M_1 &= \frac{C}{t_1^{2\nu+1}} \frac{2^{\nu+\frac{1}{2}}}{\Gamma(-\nu+\frac{1}{2})} \frac{-i\,2(-\nu+\frac{1}{2})}{t_1}, \\ M_2 &= \frac{C}{t_1^{2\nu+1}} \frac{2^{\nu+\frac{1}{2}}}{\Gamma(-\nu+\frac{1}{2})} \frac{1+\nu}{(3+2\nu)} \left(1+\nu-\frac{2}{t_1^2}(1+2\nu)(3+2\nu)\right). \end{aligned} \tag{3.18}$$

Note that it is clear that the Green function does not vanish identically for $k = 0$ for arbitrary t_1, v, since these moments do not vanish.

3.3 Recursive numerical construction of the Green function

It is easy to set up an algorithm in Mathematica to evaluate the moments recursively as discussed in section 2. This algorithm is used to evaluate 56 moments of the function $C_2(\omega)$. From (2.18) we can construct the Green function to $O(v^{56})$.[3] To improve accuracy we then approximate the Green function using the (28|28)th Padé approximant. The results for the Green function are given in the 3 figures which we will discuss.

Figure 2, shows the thermalizing Green function (solid blue curve), the vacuum Green function (dot-dashed red curve), and the thermal Green function (green dashed curve), as functions of future time v. The thermalizing Green function starts close to the vacuum Green function, for small time, however it deviates away from the vacuum Green function within one horizon time. At large time, the thermalizing Green function approaches the thermal one. At $v = 0$, the thermal Green function starts at a different value than the thermalizing and the vacuum Green functions. The thermal Green function is plotted from (B.2) derived in the appendix B. Figures 2 and 3, are plotted for specific values, $\nu = \frac{2}{3}, k = \frac{\pi}{2}$ and $t_1 = -1.7$.

Figure 3 is the logarithmic plot of the absolute value of the thermalizing Green function (solid blue curve), and the imaginary part of the lowest quasinormal mode (dot-dashed red curve), $e^{-\Delta_+ v}$. It is seen that for large time, the decay of the thermalizing Green function is given by this lowest quasinormal mode. Here, large time means time of the

[2]Since we are interested only in the time dependence we are ignoring overall proportionality constants in the Green function.

[3]We stopped at this order in moments since we found that for times $v = 5$ in horizon units the Green function evaluated converged to high degree of accuracy.

JHEP07(2015)041

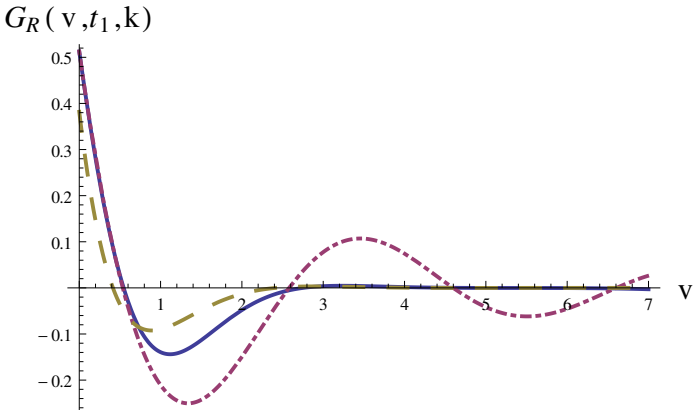

Figure 2. The thermalizing (solid blue curve), vacuum (dot-dashed red curve) and thermal (dashed green curves) Green functions are plotted as functions of future time, v, for fixed values, $\nu = \frac{2}{3}, k = \frac{\pi}{2}$ and $t_1 = -1.7$.

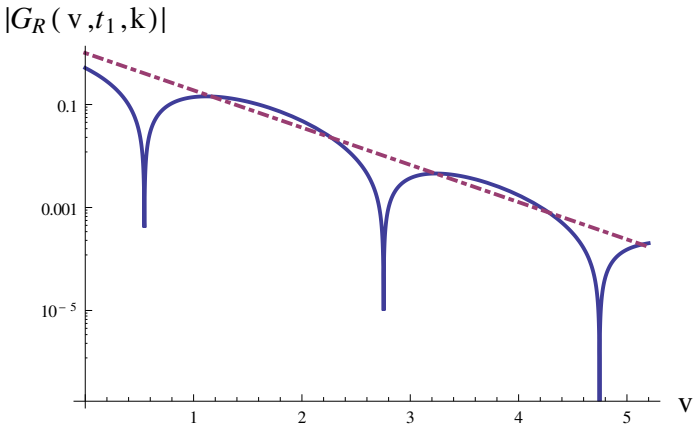

Figure 3. The logarithmic plot of the absolute value of the thermalizing Green function is given by the solid blue curve, for fixed values, $\nu = \frac{2}{3}, k = \frac{\pi}{2}$ and $t_1 = -1.7$. The dot-dashed red line gives the lowest quasinormal mode of the thermal Green function.

order of a few horizon radii, as can be seen from the plot. It is important to note that thermalization, i.e. decay of thermalizing Green function follows the lowest quasinormal mode, is achieved within a few ($\sim O(1)$) horizon radii. The dips in the plot are the points where the thermalizing Green function crosses the time axis in figure 2, and indicates the oscillations of this Green function. Figures 2 and 3 reproduce those found in [23] by the direct numerical integration of the differential equation (3.2).

Lastly, in figure 4, the thermalizing (red dots) and the thermal (solid blue curve) Green function are plotted as function of k. The value of the thermalizing Green function close to $k = 0$ is non zero, as expected from the earlier discussion in around (3.18). Also, the values of the thermalizing and the thermal Green functions are close to each other near $k = 0$. This figure is plotted for specific values, $\nu = \frac{2}{3}, t_1 = -2$ and $t_2 = 5$.

JHEP07(2015)041

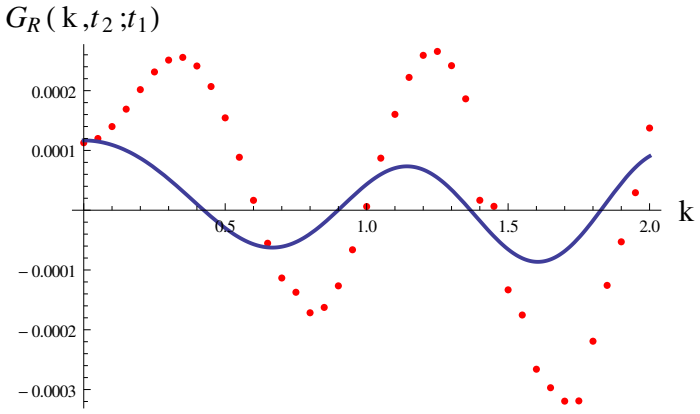

Figure 4. The thermalizing and thermal Green functions as functions of k are given by the red dots and solid blue curve, respectively, for fixed values, $\nu = \frac{2}{3}, t_1 = -2$ and $t_2 = 5$. From the plot it is seen that values of the thermalizing and thermal Green function are close to each other near $k = 0$.

4 Long time behaviour of the Green function

It is clear from the expression for the Green function given in (2.18), that for obtaining the long time behaviour of the Green function we need to evaluate moments M_n for large values of n. Form the recursive relations for the moments in (2.14) we see that this can be done if we implement the matching of the wave functions to order z^n. This in turn implies that we need the knowledge of the less dominant wave function in (2.6) Φ^+ defined by

$$\Phi^+(\omega, k, z) = \sum_{n=0}^{\infty} z^{\Delta_+} A_n(\omega, k, z) z^n, \tag{4.1}$$

closer to the horizon. This is because the coefficients of z^n for large values of n will be determined by the singular behaviour at the horizon. The behaviour of this wave function near the horizon can be determined by the general properties of solutions of wave equations in AdS black holes. Using this information we will show that the long time behaviour of the Green function is determined by the first quasinormal mode. We will first demonstrate this for the case of the minimally coupled scalar in AdS_3 Vaidya. This is easy to do explicitly since, the wave function $\Phi^{\mathrm{BTZ}(+)}$ is known in closed form. We will then show in general that the long time behaviour of the Green function is determined by the first quasinormal mode of the wave functions in the corresponding black hole background.

4.1 Green function in AdS_3 Vaidya

From the preceding discussion we need to examine the behaviour of the function $\Phi^+(\omega, k, z)$ close to the horizon. For the case of the minimally coupled scalar in the BTZ black hole this function is known in closed form (3.14) and is given by

$$\Phi^{\mathrm{BTZ}(+)}(\omega, k, z) = z^{\Delta_+}(1+z)^{-i\omega}{}_2F_1\left(\frac{1}{2}(\Delta_+ - i(\omega+k)), \frac{1}{2}(\Delta_+ - i(\omega-k)), \Delta_+, z^2\right). \tag{4.2}$$

JHEP07(2015)041

The near horizon limit of this wave function can be easily determined from the properties of the hypergeometric function given in (A.1). We see that the singular behaviour near $z = 1$ is given by

$$\Phi^{\mathrm{BTZ}(+)}(\omega, k, z) \sim (1-z)^{i\omega} \frac{\Gamma(\Delta_+)\Gamma(-i\omega)}{\Gamma(\frac{1}{2}(\Delta_+ - i(\omega-k)))\Gamma(\frac{1}{2}(\Delta_+ - i(\omega+k)))}. \tag{4.3}$$

This equation will serve as the starting point of obtaining the long term behaviour of the Green function. It is important to note that the mode Φ^+ vanishes near the horizon when the frequency is given by

$$\omega_n^{\pm} = -i\Delta_+ - 2ni \pm k, \qquad n = 0, 1, 2, \cdots . \tag{4.4}$$

These are the quasinormal modes of the minimally coupled scalar in the BTZ black hole [32]. Also note that these modes are located in the lower half ω-plane. We now impose the matching condition at $v = 0$. This will lead to the following equation

$$\begin{aligned} &C \frac{|k|^{\nu+\frac{1}{2}}}{(t_1^2 + 2|t_1|z)^{\frac{(2\nu+1)}{4}}} J_{-\nu-\frac{1}{2}}\left(|k|\sqrt{t_1^2+2|t_1|z}\right) \\ &\sim \int_{-\infty}^{\infty} d\omega C_2(\omega)(1-z)^{-i\omega} \frac{\Gamma(\Delta_+)\Gamma(-i\omega)}{\Gamma(\frac{1}{2}(\Delta_+ - i(\omega-k)))\Gamma(\frac{1}{2}(\Delta_+ - i(\omega+k)))}. \end{aligned} \tag{4.5}$$

We expect this approximation near the horizon to estimate the behaviour of the moments suitable to obtain long time behaviour of the Green function. We can now solve for $C_2(\omega)$ by substituting

$$y = \ln(1-z), \tag{4.6}$$

and multiplying both sides of the equation in (4.5) by $e^{-i\omega' y}$ and formally integrating over y from $-\infty$ to ∞.[4] This leads to the following expression for $C_2(\omega)$

$$C_2(\omega) \sim \tilde{I}(\omega, k) \frac{\Gamma(\frac{1}{2}(\Delta_+ - i(\omega-k)))\Gamma(\frac{1}{2}(\Delta_+ - i(\omega+k)))}{\Gamma(\Delta_+)\Gamma(-i\omega)}, \tag{4.7}$$

where

$$\tilde{I}(\omega, k) = \frac{C}{2\pi} \int_{-\infty}^{\infty} dy \frac{|k|^{\nu+\frac{1}{2}}}{(t_1^2 + 2|t_1|z)^{\frac{2\nu+1}{4}}} J_{-\nu-1/2}\left(|k|\sqrt{t^2+2|t_1|z}\right) e^{-i\omega y}. \tag{4.8}$$

Finally the Green function is given by

$$\begin{aligned} G_R(k, v, t_1) = &\int_{-\infty}^{\infty} d\omega e^{-i\omega v} C_2(\omega) = \\ &\int_{-\infty}^{\infty} d\omega e^{-i\omega v} \frac{\Gamma(\frac{1}{2}(\Delta_+ - i(\omega-k)))\Gamma(\frac{1}{2}(\Delta_+ - i(\omega+k)))}{\Gamma(\Delta_+)\Gamma(-i\omega)} \tilde{I}(\omega, k). \end{aligned} \tag{4.9}$$

Note that the factor multiplying $\tilde{I}(\omega, k)$ in (4.9) is a function of ω such that for $\omega \to -i\infty$ it behaves as

$$\begin{aligned} \lim_{\omega \to -i\infty} H(\omega, k) &= \lim_{\omega \to -i\infty} \frac{\Gamma(\frac{1}{2}(\Delta_+ - i(\omega-k)))\Gamma(\frac{1}{2}(\Delta_+ - i(\omega+k)))}{\Gamma(\Delta_+)\Gamma(-i\omega)}, \\ &\sim e^{+i\omega \ln 2}(\omega)^{\nu+\frac{1}{2}}. \end{aligned} \tag{4.10}$$

[4] Though the range of y is restricted from $-\infty$ to 0, we are extending this range formally to obtain C_2.

JHEP07(2015)041

$\tilde{I}(\omega,k)$ is essentially a Fourier transform of the Bessel function. We assume that this is analytic in the lower half ω-plane and grows *at the most* exponentially in ω as $\omega \to -i\infty$, given by

$$\lim_{\omega\to -i\infty} \tilde{I}(\omega,k) < e^{i\omega M}. \tag{4.11}$$

Here $M > 0$ is a fixed constant. With these assumptions and the behaviour in (4.10) we see that integrand in (4.9) goes to zero in the limit $\omega \to -i\infty$ for sufficiently large but fixed $v > 0$. This is because of the exponentially dying term $e^{-i\omega v}$ in the integrand of (4.9). Therefore the integral can be performed by completing the contour in the lower half ω-plane. Then the integral localizes to a sum over the poles of the Gamma functions. The poles of the Gamma functions are at the quasinormal modes given by (4.4). The result of the integral then reduces to

$$G(k,v,t_1) \sim \sum_{n=0,\alpha=\pm}^{\infty} e^{-i\omega_n^\alpha v}\tilde{I}(\omega_n^\alpha,k)(-2\pi i\,\text{Residue}_{\omega=\omega_n^\alpha} H(\omega,k)). \tag{4.12}$$

It is now clear from (4.12) that the long time behaviour of the Green function is determined by the lowest quasinormal mode as we have seen in our explicit numerical evaluation of the Green function. The decay of the Green function is controlled by the imaginary part of the lowest quasinormal mode and the period of oscillation is determined by the real part of the lowest quasinormal mode. Note also from (4.12) we see that since the expression involves a sum over all the quasinormal modes, the rough time scale over which the lowest quasinormal mode takes over is of the order of a few horizon times. This is also clearly seen in the numerical evaluation of the Green function. It is important to note that the starting point of the analysis was the behaviour of $\Phi^{\text{BTZ}(+)}$ near the horizon given in (4.3), which vanished at frequencies determined by the quasinormal mode spectrum in the lower half ω-plane.

4.2 Green function in AdS_{d+1} Vaidya

Using the intuition gained by the explicit solutions of the minimally coupled scalar in the BTZ black hole we now generalize the discussion. We show that the long time behaviour of the retarded Green function in arbitrary AdS_{d+1} Vaidya background is determined by the lowest quasinormal mode of the corresponding bulk field.

Consider the differential equation given in (2.1) for the minimally coupled scalar in the AdS_{d+1} Vaidya for $v > 0$. Substituting

$$\phi(v,k,z) = \Phi_\omega(z,k)e^{-i\omega v}, \tag{4.13}$$

we obtain

$$(1-z^d)\partial_z^2\Phi_\omega - i\omega\left(\frac{\Phi_\omega}{z} - 2\partial_z\Phi_\omega\right) - \left(dz^{d-1} + \frac{1}{z}(1-z^d)\right)\partial_z\Phi_\omega - \left(\frac{m^2}{z^2}+k^2\right)\Phi_\omega = 0. \tag{4.14}$$

This equation has two regular singular points, $z = 0$ and $z = 1$, corresponding to the boundary and the horizon of the black hole. One can set up a Frobenius solution around

JHEP07(2015)041

either $z=0$ or $z=1$. Let the two independent solutions around $z=0$ be Φ_ω^+ and Φ_ω^-. From the indicial equation for the expansion at $z=0$ we know that these solutions behave as follows[5]

$$\lim_{z\to 0}\Phi_\omega^+(z,k)\sim z^{\Delta_+},\qquad \lim_{z\to 0}\Phi_\omega^-(z,k)\sim z^{\Delta_-}. \tag{4.15}$$

Therefore Φ_ω^- is the dominant singular mode at the boundary. Similarly one can set up an expansion around $z=1$, let the two independent solutions around $z=1$ be $\Phi_\omega^{\rm in}$ and $\Phi_\omega^{\rm out}$. It is easy to see from the indicial equation around $z=1$, that their behaviour near $z=1$ is given by

$$\lim_{z\to 1}\Phi_\omega^{\rm out}(z,k)\sim e^{i\frac{2\omega}{d}\ln(1-z)},\qquad \lim_{z\to 1}\Phi_\omega^{\rm in}(z,k)\sim (1-z)^0. \tag{4.16}$$

The reason we have labeled these solutions as in and out is because they correspond to the ingoing and outgoing solutions when these wave functions are transformed to the t,z coordinates. To see this note that the coordinate transformation near $z=1$ can be obtained by integrating (1.3). This is given by

$$v\sim t+\frac{1}{d}\ln(1-z). \tag{4.17}$$

Substituting this coordinate transformation we obtain the corresponding wave functions in the t,z coordinates

$$\begin{aligned}\phi_\omega^{\rm out}(v,z)&=e^{-i\omega v}\Phi_\omega^{\rm in}(z,k)\sim e^{-i\omega t}(1-z)^{\frac{i\omega}{d}},\\ \phi_\omega^{\rm in}(v,z)&=e^{-i\omega v}\Phi_\omega^{\rm out}(z,k)\sim e^{-i\omega t}(1-z)^{-\frac{i\omega}{d}}.\end{aligned} \tag{4.18}$$

Now we have 2 sets of linearly independent solutions $\{\Phi_\omega^+,\Phi_\omega^-\}$ and $\{\Phi_\omega^{\rm in},\Phi_\omega^{\rm out}\}$. Therefore by the uniqueness theorem of second order ordinary linear differential equations we should be able to express one set in terms of the other as linear combinations. Let us write

$$\begin{aligned}\Phi_\omega^{\rm out}(z,k)&=M_{11}(\omega,k)\Phi_\omega^+(z,k)+M_{12}(\omega,k)\Phi_\omega^-(z,k),\\ \Phi_\omega^{\rm in}(z,k)&=M_{21}(\omega,k)\Phi_\omega^+(z,k)+M_{22}(\omega,k)\Phi_\omega^-(z,k).\end{aligned} \tag{4.19}$$

Let us now use the definition of quasinormal modes to obtain some information of the coefficients M_{12} and M_{22}. We have seen that $\Phi_\omega^{\rm in},\Phi_\omega^{\rm out}$ correspond to the ingoing and outgoing modes in the t,z coordinates. Now by definition quasinormal modes are those values of frequencies for which these modes obey Dirichlet boundary conditions at the asymptotic boundary. This implies that the more dominant mode proportional to Φ_ω^- should vanish at these frequencies. Thus we have the equation

$$M_{12}(\omega_n^{\rm out},k)=0,\qquad M_{22}(\omega_n^{\rm in},k)=0, \tag{4.20}$$

where $\omega_n^{\rm out}$ are the quasinormal frequencies which lie in the upper half ω-plane for the outgoing modes and $\omega_n^{\rm in}$ are the quasinormal frequencies which lie in the lower half ω-plane for the ingoing modes [32, 33]. Let us invert the equation (4.19), we obtain

$$\begin{pmatrix}\Phi_\omega^+(z,k)\\ \Phi_\omega^-(z,k)\end{pmatrix}=\frac{1}{\det M}\begin{pmatrix}M_{22}&-M_{12}\\ -M_{21}&M_{11}\end{pmatrix}\begin{pmatrix}\Phi_\omega^{\rm out}(z,k)\\ \Phi_\omega^{\rm in}(z,k)\end{pmatrix}. \tag{4.21}$$

[5] We have assumed that the roots of the indicial equation do not differ by an integer. The discussion can be easily generalized in case they do.

JHEP07(2015)041

Note that the inverse exists that is $\det M \neq 0$. This is because Φ^+_ω and Φ^-_ω can be written as linear combinations of $\Phi^{\rm in}_\omega$ and $\Phi^{\rm out}_\omega$. We can now easily read out the near horizon behaviour of the solution Φ^+_ω from the above equation. The singular behaviour of Φ^+_ω is given by

$$\Phi^+_\omega(z,k) = \frac{1}{\det M}\left(M_{22}(\omega,k)\Phi^{\rm out}_\omega(z,k) - M_{12}(\omega,k)\Phi^{\rm in}_\omega(z,k)\right), \tag{4.22}$$
$$\Phi^+_\omega(z,k)|_{z\to 1} \sim \frac{1}{\det \mathrm{M}} M_{22}(\omega,k)(1-z)^{i\frac{2\omega}{d}}.$$

Here we have used the near horizon behaviour given in (4.16). Now $M_{22}(\omega,k)$ vanishes at $\omega = \omega^{\rm in}_n$, with zeros in the lower half plane. This is the general form of the equation (4.3) seen explicitly for the case of the BTZ black hole for black holes in AdS_{d+1}. Note that we arrived at this result from the general definition of quasi-normal modes. From this point onwards we can follow the rest of the argument in section 4.1 to arrive at the conclusion that the long time behaviour is determined by the leading quasinormal mode. In general the gaps between quasinormal modes are of the order of horizon scales. Therefore we expect the leading behaviour to set in order of a few horizon times. Though here we have used the minimally coupled scalar to demonstrate our argument for simplicity, the analysis can be carried out for other fields. The steps involved will result in similar equations. We will see this explicitly for the vector fluctuations of the metric in the subsequent section.

This concludes our general argument of why the long time behaviour is determined by the leading quasinormal mode. Thus any retarded correlator which is used to probe the onset of thermalization caused due to injection of energy at an instance of time in the field theory will decay with the time scale set by the first quasinormal mode. In [34] it was conjectured that thermalization time scales in the field theory are determined by quasinormal modes. We have shown that the time dependent Green functions considered in this paper provide an explicit realization of this statement. From our general argument we expect this to be true for correlators whose lowest quasinormal modes are determined by hydrodynamics if the probing momentum scales are sufficiently small. In the next section we will verify this expectation for stress tensor correlators in $\mathcal{N} = 4$ Yang-Mills whose lowest quasinormal mode is sensitive to the shear viscosity.

5 Thermalization in AdS_5 Vaidya

In this section we study the thermalization of the retarded two point functions in the thin shell AdS_5 Vaidya geometry. We first consider the equation satisfied by the spin 2 metric fluctuation $h_{x^1x^2}$. This fluctuation, perpendicular to the momentum k which is along the x^3 direction, forms the shear spin 2 mode. Evaluating the retarded Green function holographically for this mode provides information of the retarded two point function of the stress tensor $\langle T_{x^1x^2}T_{x^1x^2}\rangle$, for the strongly coupled $\mathcal{N} = 4$ Yang-Mills.[6] The lowest quasinormal mode of shear fluctuations of the metric has been studied earlier

[6] Metric perturbations for spherical shell collapse was studied in [35]. Non-equilibrium Green function corresponding to the shear correlator was studied earlier by a complementary approach by examining backgrounds perturbed by hydrodynamic modes [36, 37].

JHEP07(2015)041

in [27] numerically. We see our results are consistent with this earlier calculation. The more interesting metric fluctuation to consider is $h_{x^1x^3}$. It is known that this mode admits a hydrodynamic quasinormal mode in the AdS_5 black hole for small momentum [28]. This mode appears as a pole in the thermal two point function of the stress tensor $\langle T_{x^1x^3} T_{x^1x^3}\rangle$. We will implement the recursion method numerically and evaluate the thermalizing Green function for various values of small momentum k. From the long time behaviour of the Green function we show that this Green function relaxes by the hydrodynamic quasinormal mode. This enables us to read out the universal shear viscosity to entropy density ratio from a time dependent process.

The thin shell AdS-Vaidya metric in 5 dimensions is given by,

$$ds^2 = \frac{1}{z^2}\left[-h(v,z)dv^2 - 2dzdv + d\vec{x}^2\right], \tag{5.1}$$

$$h(v,z) = 1 - \theta(v) z^4, \tag{5.2}$$

here, $\vec{x}$ is a 3 vector, with components, x^i, where $i = 1, 2, 3$. The x^i's parametrize the spatial directions in the dual field theory. The transformation which reduces the $v > 0$ part of the above metric to the AdS_5 black hole metric in Poincaré co-ordinates is given by

$$dv = dt - \frac{dz}{1 - z^4}. \tag{5.3}$$

In these coordinates we obtain the planar black hole metric in AdS_5, for $v > 0$,

$$ds^2 = \frac{1}{z^2}\left[-(1 - z^4)dt^2 + \frac{dz^2}{1 - z^4} + d\vec{x}^2\right]. \tag{5.4}$$

Here again the radius of AdS as well as the black hole has been set to unity. The temperature of the black hole is then given by

$$T = \frac{1}{\pi}. \tag{5.5}$$

To study two point functions of the stress energy tensor of the boundary field theory we consider small perturbations to the background metric, $g^{(0)}_{\mu\nu}$, of (5.1), $g_{\mu\nu} = g^{(0)}_{\mu\nu} + h_{\mu\nu}$. The differential equations satisfied by the metric perturbations are obtained by linearizing the Einstein's equations which are given by

$$\mathcal{R}_{\mu\nu} = -4\, g_{\mu\nu}. \tag{5.6}$$

Here $\mathcal{R}_{\mu\nu}$ is the Ricci tensor and the value of cosmological constant, Λ, has been set to $\Lambda = -6$, in units of AdS radius. The linearized Einstein's equations are given by

$$\mathcal{R}^{(1)}_{\mu\nu} = -4\, h_{\mu\nu}, \tag{5.7}$$

where $\mathcal{R}^{(1)}_{\mu\nu}$ is the linearized Ricci curvature.

JHEP07(2015)041

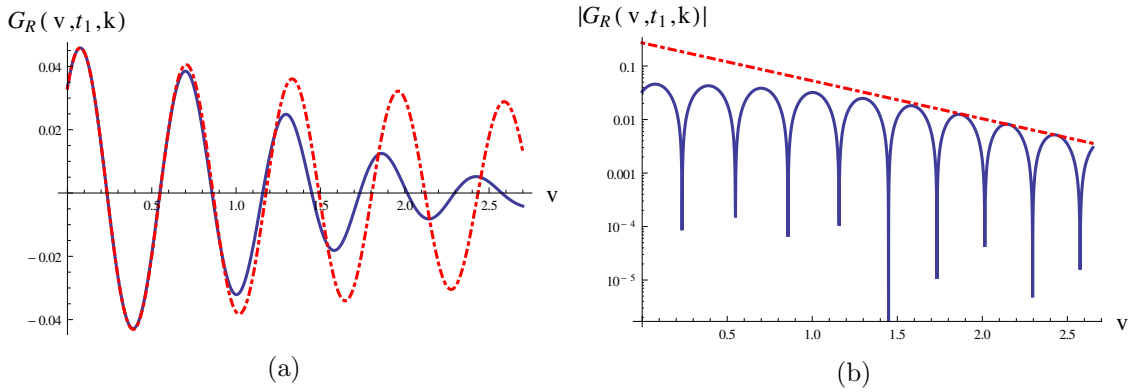

Figure 5. Figure (a) shows the thermalizing (solid blue curve), and vacuum (dot-dashed red curve) Green functions for the shear mode. Figure (b) shows the logarithmic plot of the absolute value of the thermalizing Green function. Plots are for values $t_1 = -15$ and $k = 10$.

5.1 Spin 2 metric perturbations

First, we consider the case when only the scalar mode of metric perturbation, $h_{x_1x_2}$, is turned on. We substitute the ansatz $h_{x^1x^2}(t, x^3, z) = e^{-i\omega t + ikx^3}\tilde{h}_{x^1x^2}(z)$ in (5.7). Here, the momentum is chosen to be along the x^3 direction. After the redefinition $\Phi(z) = z^2\tilde{h}_{x^1x^2}(z)$ we obtain the following equation from (5.7),

$$v < 0: \qquad z^2\Phi'' - z(3 - 2i\omega z)\Phi' - (k^2z^2 + 3i\omega z)\Phi = 0, \tag{5.8}$$

$$v > 0: \quad z^2(1 - z^4)\Phi'' - z(3 + z^4 - 2i\omega z)\Phi' - (k^2z^2 + 3i\omega z)\Phi = 0, \tag{5.9}$$

where the prime means derivative with respect to z. Note that as expected these are the equations of the minimally coupled massless scalar in the AdS_5 background for $v < 0$ and the AdS_5 black hole background for $v > 0$.

Solution for $v < 0$. In appendix C we have obtained the solution which satisfies the boundary condition (2.5) for a minimally coupled massive scalar in AdS_5. On setting the parameter $m^2 = 3$ or $\nu = 2$ in (C.1), the equation reduces to (5.8). Therefore we can read out the solution in mixed Fourier space which satisfies the required boundary condition from (C.18). This is given by

$$\Phi^{\mathrm{AdS}}(v, k, z; t_1) = G_R^{\mathrm{AdS}}(v, k, z; t_1) = \theta(v - t_1)2^{-\frac{3}{2}}\sqrt{\pi}\times \tag{5.10}$$
$$\left(\frac{k}{\sqrt{(v - t_1)^2 + 2(v - t_1)z}}\right)^{\frac{5}{2}} z^4 J_{-\frac{5}{2}}\left(k\sqrt{(v - t_1)^2 + 2(v - t_1)z}\right).$$

Solution for $v > 0$. Unlike the case of the BTZ black hole, closed form solutions to minimally coupled scalar in the AdS_5 black holes are not available. However the recursive method we developed in section 2 just relies on information of the Frobenius expansion of the solution near the boundary. The roots of the indicial equation of (5.9) are given by $\Delta_\pm = 4, 0$. As discussed earlier to obtain the retarded Green function we need to obtain the Frobenius solution with the less dominant mode, that is with $\Delta_+ = 4$. The recursion

JHEP07(2015)041

relations for the coefficients a_n^js defined in (2.10), necessary for the construction of the solution in the region $v > 0$, are given by the following equations with $a_0^0 = 1$,

$$\begin{aligned}
&a_1^0 = 0, \qquad a_1^1 = -ia_0^0, \\
&a_2^0 = \frac{k^2 a_0^0}{12}, \quad a_2^1 = 0, \qquad a_2^2 = \frac{-i7a_1^1}{12}, \\
&a_3^0 = 0, \qquad a_3^1 = \frac{k^2 a_1^1 - i9a_2^0}{21}, \quad a_3^2 = 0, \quad a_3^3 = \frac{-i9a_2^2}{21},
\end{aligned} \tag{5.11}$$

and, for $n \geq 4$,

$$\begin{aligned}
a_n^0 &= \frac{k^2 a_{n-2}^0 + n^2 a_{n-4}^0}{n(n+4)}, \\
a_n^j &= \frac{-i(2n+3)a_{n-1}^{j-1} + k^2 a_{n-2}^j + n^2 a_{n-4}^j}{n(n+4)}; \quad j = 1, 2, \ldots, n-4, \\
a_n^j &= \frac{-i(2n+3)a_{n-1}^{j-1} + k^2 a_{n-2}^j}{n(n+4)}; \qquad j = n-3, n-2, \\
a_n^j &= \frac{-i(2n+3)a_{n-1}^{j-1}}{n(n+4)}; \qquad j = n-1, n.
\end{aligned} \tag{5.12}$$

We can now extract the moments of the Green function by substituting the values of a_n^j determined from (5.11), (5.12) into (2.14). The values of the coefficients $\tilde{J}_n$ in (2.14) can be obtained from the recursion relation (D.4) with $\nu = 2$. Finally the retarded Green function is constructed using (2.18). This procedure is clearly algorithmic and can be easily implemented numerically. Using Mathematica we implemented this procedure of obtaining the Green function. We have evaluated up to 200 moments $C_2(\omega)$ and the Green function is constructed to $O(v^{200})$ in future time, v. We then approximated the Green function by the (100|100) Padé Approximant for better accuracy. For the values of k studied, 200 moments were sufficient to obtain convergent results.

Figure 5a shows the thermalizing Green function (solid blue curve) for $t_1 = -15$ and a particular value of $k = 10$. As expected, the thermalizing Green function starts close to the vacuum Green function (red dot-dashed curve) at small time, and deviates from it within one horizon time. From the logarithmic plot, figure 5b the slope as shown by the dot-dashed red line of the thermalizing Green function (solid blue curve) is measured at large time, i.e. at time of the order of a few horizon radius. This slope gives the negative imaginary part of the lowest quasinormal mode ($-\mathrm{Im}\,\omega$), as shown in section 4. From the gaps between consecutive zeroes of the thermalizing Green function, real part of ω can be calculated using, $\mathrm{Re}\,\omega = \pi/\mathrm{gap}$. The values of real and imaginary part of ω, for several values of k, are listed in table 1. These values agree with figures 5, 6 of [27] where the numerical values of the real and imaginary part of the quasinormal modes for the minimally coupled scalar with $\Delta = 4$ in AdS_5 were obtained for various values of k. To compare our results to that of figures 5,6 of [27], note that we need to perform the following scalings $k^{\text{ours}} = 2q^{\text{theirs}}, \omega^{\text{ours}} = 2\omega^{\text{theirs}}$. As a simple check note that $k^{\text{ours}} = 10$ corresponds to $q^{\text{theirs}} = 5$, looking at their figure 6 we note that $\mathrm{Im}\,\omega^{\text{theirs}} = .8$ which corresponds to

JHEP07(2015)041

k	Re ω	$-$Im ω
7.0	8.34	1.90
7.5	8.84	1.77
8.0	9.29	1.76
8.5	9.80	1.78
9.0	10.28	1.76
9.5	10.72	1.63
10.0	11.21	1.63
10.5	11.70	1.52
11.0	12.22	1.55

Table 1. Values of the real and imaginary part of the lowest quasinormal modes, $-\mathrm{Im}\,\omega$, calculated from the large time behaviour of the thermalizing Green function, for several values of momentum, k, and fixed value of $t_1 = -15$.

$\mathrm{Im}\,\omega^{\mathrm{ours}} = 1.6$ which agrees with our result in table 1. Similarly note that for small values of q^{theirs}, the value of $\mathrm{Re}\,\omega^{\mathrm{theirs}}$ is above the 45° line. This is also the case from our results in table 1.

5.2 Vector metric perturbations and shear viscosity

It is known that vector metric perturbations $h_{x^1x^3}, h_{tx^1}$ in the AdS_5 black hole with momentum along the x^3 direction admits a hydrodynamic mode at small momentum in addition to the usual gapped quasinormal frequencies [28]. The hydrodynamic quasinormal mode corresponds to the hydrodynamic pole in the thermal correlator $\langle T_{tx^1} T_{tx^1}\rangle$. This was used to read out the ratio of shear viscosity to entropy density in [28]. Using the methods developed in this paper we can evaluate the time dependent thermalizing retarded two point function $\langle T_{tx^1} T_{tx^1}\rangle$ in the AdS_5 thin shell Vaidya background. From the general analysis of section 4 we expect that the time dependent Green function in the AdS_5 thin shell Vaidya background should relax to equilibrium by the hydrodynamic quasinormal mode. Therefore from the decay it should be possible to read out the ratio of shear viscosity to entropy density from a dynamical Green function. In this section we perform this analysis using the methods developed in this paper and obtain the universal ratio of shear viscosity to entropy density.[7]

We first turn on the following metric fluctuations with momentum along the x^3 direction,

$$h_{vx^1}(t, x^3, z) = e^{-i\omega t + ikx^3}\tilde{h}_{vx^1}(z), \qquad h_{x^1x^3}(t, x^3, z) = e^{-i\omega t + ikx^3}\tilde{h}_{x^1x^3}(z). \tag{5.13}$$

We can obtain the linearized equations of motion from (5.7). Redefining the fields as,

$$H_v(z) = z^2\tilde{h}_{vx^1}(z), \qquad H_3(z) = z^2\tilde{h}_{x^1x^3}(z), \tag{5.14}$$

[7] As far as the authors are aware this is the first instance where the universal ratio of shear viscosity to entropy density is obtained from a time dependent process.

JHEP07(2015)041

we obtain the following coupled equations in the AdS_5 background before the collapse of the thin shell, $v < 0$,

$$\begin{aligned} H_v'' - \frac{3}{z}H_v' + ikH_3' &= 0, \\ H_v'' + \left(-\frac{3}{z} + i\omega\right)H_v' - k^2 H_v - k\omega H_3 &= 0, \\ H_3'' + \left(-\frac{3}{z} + 2i\omega\right)H_3' - \frac{3i\omega}{z}H_3 + ikH_v' - \frac{3ik}{z}H_v &= 0. \end{aligned} \tag{5.15}$$

After the formation of the AdS_5 black hole for $v > 0$, the equations are given by

$$\begin{aligned} H_v'' - \frac{3}{z}H_v' + ikH_3' &= 0, \\ H_v'' + \frac{1}{f}\left(-\frac{3-3z^4}{z} + i\omega\right)H_v' - \frac{k^2}{f}H_v - \frac{k\omega}{f}H_3 &= 0, \\ H_3'' + \frac{1}{f}\left(-\frac{3+z^4}{z} + 2i\omega\right)H_3' - \frac{3i\omega}{zf}H_3 + \frac{ik}{f}H_v' - \frac{3ik}{zf}H_v &= 0, \end{aligned} \tag{5.16}$$

where $f = 1 - z^4$. To decouple the above differential equations we define

$$H_v' = p_v, \tag{5.17}$$

then the equations reduce to,

$$v < 0: \quad z^2 p_v'' + z(-3 + 2i\omega z)p_v' - (-3 + k^2 z^2 + 3i\omega z)p_v = 0, \tag{5.18}$$

$$v > 0: \quad z^2(1-z^4)p_v'' + z(-3 - z^4 + 2i\omega z)p_v' + (3 - k^2 z^2 + 9z^4 - 3i\omega z)p_v = 0. \tag{5.19}$$

Solution in AdS_5: $v < 0$. We see that on substituting $m^2 = 0$, i.e. $\nu = 1$ in (C.1), the equation reduces to (5.18). Therefore we can read out the solution in mixed Fourier space which satisfies the boundary condition (2.5) from (C.18). This is given by

$$\begin{aligned} p_v^{\rm AdS}(v,k,z;t_1) = G_R^{\rm AdS}(v,k,z;t_1) = \\ \theta(v-t_1)2^{-\frac{1}{2}}\sqrt{\pi}\left(\frac{k}{\sqrt{(v-t_1)^2 + 2(v-t_1)z}}\right)^{\frac{3}{2}} z^3 J_{-\frac{3}{2}}\left(k\sqrt{(v-t_1)^2 + 2(v-t_1)z}\right). \end{aligned} \tag{5.20}$$

Solution for AdS_5 black hole: $v > 0$. We again use the Frobenius expansion around the boundary $z = 0$ to solve (5.19). We obtain the following recursion relation for a_n^j for the the root $\Delta_+ = 3$ of the indicial equation where $a_0^0 = 1$,

$$\begin{aligned} a_1^0 &= 0, & a_1^1 &= -ia_0^0, & & \\ a_2^0 &= \frac{k^2 a_0^0}{8}, & a_2^1 &= 0, & a_2^2 &= \frac{-i5a_1^1}{8}, \\ a_3^0 &= 0, & a_3^1 &= \frac{k^2 a_1^1 - i7a_2^0}{15}, & a_3^2 &= 0, \quad a_3^3 = \frac{-i7a_2^2}{15}, \end{aligned} \tag{5.21}$$

JHEP07(2015)041

and, for $n \geq 4$,

$$
\begin{aligned}
a_n^0 &= \frac{k^2 a_{n-2}^0 + (n^2-2n-8)a_{n-4}^0}{n(n+2)}, && \\
a_n^j &= \frac{-i(2n+1)a_{n-1}^{j-1} + k^2 a_{n-2}^j + (n^2-2n-8)a_{n-4}^j}{n(n+2)}; && j = 1, 2, \ldots, n-4, \\
a_n^j &= \frac{-i(2n+1)a_{n-1}^{j-1} + k^2 a_{n-2}^j}{n(n+2)}; && j = n-3, n-2, \\
a_n^j &= \frac{-i(2n+1)a_{n-1}^{j-1}}{n(n+2)}; && j = n-1, n.
\end{aligned}
\tag{5.22}
$$

Note that a_n^j, defined above determine the Frobenius expansion around the boundary for the differential equation for p_v given in (5.19). We can implement the matching conditions (2.7) on the function p_v and construct the Green function as done in the previous examples from the values of a_n^j in (5.21) and (5.22) using the equations (2.14) and (2.18). The time dependence of the Green function corresponding to the mode p_v is proportional to the Green function $\langle T_{tx^1} T_{tx^1} \rangle$. This reason is as follows: note that the vector fluctuation h_{vx^1} reduces to h_{tx_1} at the boundary since the coordinate v equals time t at the boundary. It is h_{tx_1} which determines the behaviour of the Green functions $\langle T_{tx^1} T_{tx^1} \rangle$. Now H_v is related to the vector fluctuation h_{vx^1} from equations (5.13) and (5.14). Finally H_v is related to p_v by the equation (5.17). This implies that the power series expansion of H_v is given by

$$
H_v = z^4 \left(\sum_{n=0}^{\infty} A_n z^n \right), \qquad A_n = \sum_{j=0}^{n} a_n^j \omega^j \tag{5.23}
$$

where a_n^j are given in (5.21) and (5.22). Note that the only difference between the mode H_v and p_v is that $\Delta_+ = 3$ for p_v while it is $\Delta_+ = 4$ for H_v. Therefore reading out the time dependence of p_v is sufficient to extract the time dependence of the two point function $\langle T_{tx^1} T_{tx^1} \rangle$.

Green function and quasinormal modes. Using the equations (5.21), (5.22), (2.14) and (D.4), with $\nu = 1$, the moments M_i are obtained. Then the thermalizing retarded Green function $\langle T_{tx^1} T_{tx^1} \rangle$ of the boundary theory, is evaluated using (2.18). We used Mathematica to evaluate up to 3500 moments $C_2(\omega)$, the results converged at this order of moments. The Green function is constructed to $O(v^{3500})$ in future time, v and then we approximated it by its (1750|1750) Padé approximant. From these moments the Green function is evaluated for various values of the momentum k.

Figure 6a shows the thermalizing Green function (solid blue curve), which starts close to the vacuum Green function (dot-dashed red curve), and deviates away from it within one horizon time.

The hydrodynamic pole of the thermal two point function $\langle T_{tx^1} T_{tx^1} \rangle$ or the quasinormal mode of the vector perturbations of the metric obeys the dispersion relation

$$
\omega = -i \frac{\eta}{sT} k^2. \tag{5.24}
$$

JHEP07(2015)041

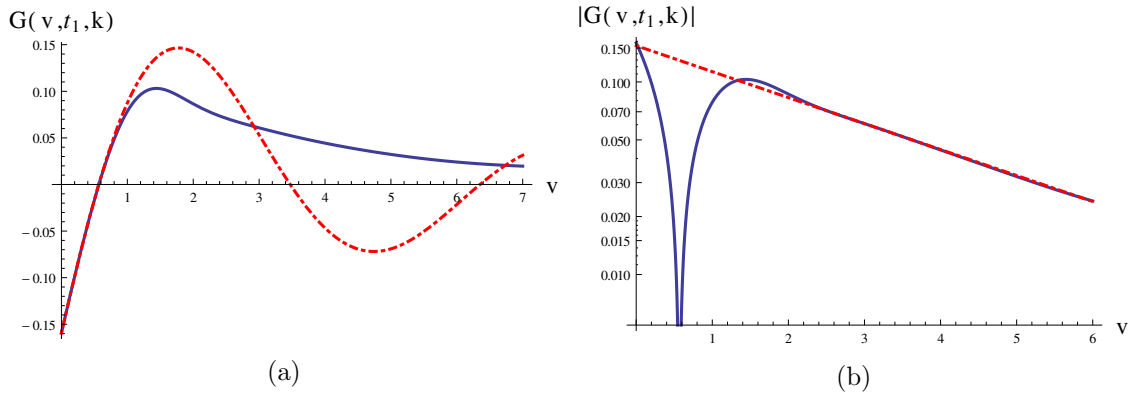

(a) (b)

Figure 6. The solid blue curve is the thermalizing Green function. In (a), the dot-dashed curve is the vacuum Green function. Figure (b) has the logarithmic plot of the absolute value of the Green function, plotted with its late time slope (red dot-dashed curve). Plots are for values, $t_1 = -5$ and $k = 1.1$.

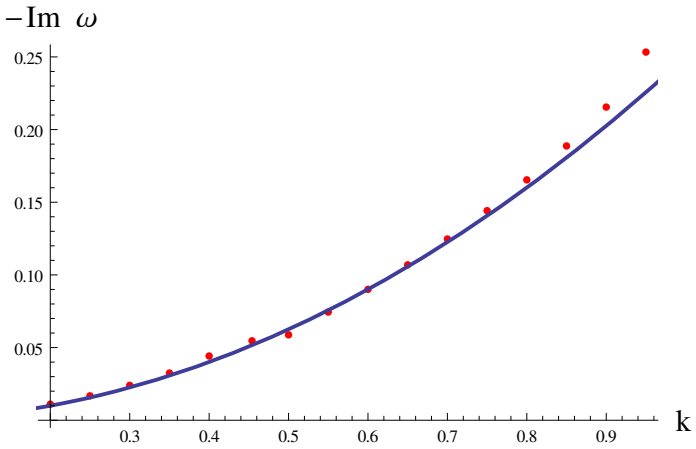

Figure 7. The red dots show the value of the hydrodynamic frequency obtained from the slope of the long time behaviour of the Green function (at $t_1 = -5$) for various values of k. The blue curve plots the expected behaviour, $-\text{Im}\ \omega = \frac{1}{4}k^2$.

η, s and T are the shear viscosity, entropy density and temperature, respectively. The universal value of η/s for the vector mode of metric perturbation is known to be $(4\pi)^{-1}$. The temperature of the AdS_5 black hole is $T = \pi^{-1}$, in which the radius of AdS and that of the horizon are normalized to unity. Therefore the dispersion relation for the hydrodynamic quasinormal frequencies is given by

$$\omega = -i\frac{k^2}{4}. \tag{5.25}$$

As discussed in section 4 the long time behaviour of the thermalizing Green function is dictated by the lowest quasinormal mode. Therefore it is possible to extract the value of the $-\text{Im}\ \omega$ from the slope of the logarithmic plot of the thermalizing Green function for $k \ll 1$ and show that it obeys the dispersion relation given in (5.25).

JHEP07(2015)041

In figure 6b, the logarithmic plot of the absolute value of the thermalizing Green function (solid blue curve) is plotted along with the line measuring the slope of its large time behaviour (dot-dashed red line). The slope of this straight line gives the value of $-\text{Im}\ \omega$. The plot is for fixed values of $t_1 = -15$ and $k = 10$. Figure 7, shows the red dots for values of $-\text{Im}\ \omega$ for several values of k obtained from Mathematica. For small k, these values lie very close to the expected parabolic behaviour (solid blue curve), predicted by the hydrodynamic dispersion relation (5.25). For larger k, these values lie inside the parabola. This behaviour agrees with figure 12 of [27] which studied this quasinormal mode for large values of k in the AdS_5 black hole.

6 Conclusions

We have developed a recursive method to obtain the time dependent Green functions in the thin shell AdS Vaidya background. Using the intuition developed from this method we showed that the long time behaviour of the Green function is determined by the lowest quasinormal mode of the corresponding black hole. Thus our analysis provides an explicit realization of the general conjecture made in [34] that time scales in thermalization are determined by the quasinormal modes. We applied the method to study Green functions in thin shell Vaidya geometries in AdS_3 and AdS_5. Using this method we obtained the universal ratio of shear viscosity to entropy density by studying the relaxation of the time dependent Green function of the vector metric perturbation in the AdS_5 Vaidya shell.

The methods developed in this paper to study time dependent Green functions can be generalized for fermion Green function which was obtained by direct numerical integration in [24]. It will be interesting to generalize this method to Vaidya shell geometries which have a finite width found in [13]. These geometries are a more accurate description of the thermalization process. The dependence of the width of the shell on the time dependence of the Green function will be interesting to extract. It is interesting to study thermalization of Green function of higher spin fields to study the spin dependence in thermalization. It is known that a non local probe like entanglement entropy is the slowest to relax to equilibrium [21]. It will be interesting to see if higher spin fields relax faster or slower compared to scalars and entanglement entropy. In this context the exact solutions to wave functions of higher spin fields found in the BTZ background [38, 39] will prove to be useful to obtain analytical results. Finally it will be useful to use these lessons learned in holography to understand time dependent Green function in conformal field theories during thermalization along the lines developed in [40].

Acknowledgments

We thank Johanna Erdmenger, Daniel Fernandez and Eugenio Megias-Fernandez for useful discussions during the initial phase of this project. We thank Sayantani Bhattacharyya, Chethan Krishnan, Kalyana Rama and Bala Sathiapalan for asking questions that clarified our understanding of the problem. We also thank Pallab Basu and Dileep Jatkar for interesting comments. S.K. thanks Shouvik Datta for help with the graphics used in the paper. We thank the participants of the Bangalore area string meeting organized by the

JHEP07(2015)041

ICTS, TIFR, the string groups of IMSc, Chennai and IIT Kanpur for opportunities to present the results at various stages of the project and the resulting discussions. Finally J.R.D. thanks Dieter Lust and the string group at Max Planck Institute for Physics, Munich for hospitality during the initial phase of this project.

A Scalar wave functions in BTZ

In this appendix we derive the scalar wave functions in the BTZ geometry as an expansion around the boundary by transforming the known wave functions which are written as expansions around the horizon. Consider the wave functions given in (3.12) which admit a natural expansion near the horizon. We can use the following transformation property of the Hypergeometric function to write it as an expansion around the boundary,

$$F(a,b,c,z) = \frac{\Gamma(c)\Gamma(c-a-b)}{\Gamma(c-a)\Gamma(c-b)}F(a,b,a+b-c+1,1-z) + (1-z)^{c-a-b}\frac{\Gamma(c)\Gamma(a+b-c)}{\Gamma(a)\Gamma(b)}F(c-a,c-b,c-a-b+1,1-z). \tag{A.1}$$

Substituting (A.1) in (3.12) we obtain

$$\Phi^{(1)}_{\omega,k}(z,v,\phi) = e^{-i\omega v+ik\phi}(1+z)^{-i\omega}\times \left[B_1(\nu,\omega,k)z^{\Delta_-}F\left(\frac{1}{2}(\Delta_- - i(\omega-k)),\frac{1}{2}(\Delta_- - i(\omega+k)),\Delta_-,z^2\right) + B_2(\nu,\omega,k)z^{\Delta_+}F\left(\frac{1}{2}(\Delta_+ - i(\omega+k)),\frac{1}{2}(\Delta_+ - i(\omega-k)),\Delta_+,z^2\right)\right], \tag{A.2}$$

$$\Phi^{(2)}_{\omega,k}(z,v,\phi) = e^{-i\omega v+ik\phi}(1-z)^{i\omega}\times \left[B_3(\nu,\omega,k)z^{\Delta_-}F\left(\frac{1}{2}(\Delta_- + i(\omega+k)),\frac{1}{2}(\Delta_- + i(\omega-k)),\Delta_-,z^2\right) + B_4(\nu,\omega,k)z^{\Delta_+}F\left(\frac{1}{2}(\Delta_+ + i(\omega-k)),\frac{1}{2}(\Delta_+ + i(\omega+k)),\Delta_+,z^2\right)\right]. \tag{A.3}$$

The coefficients B_i, $i = 1,\ldots 4$, are made up of gamma functions obtained from (A.1), and do not depend on z. The hypergeometric functions of (A.3) can further be related to the hypergeometric functions of (A.2), by the transformation,

$$F(a,b,c,z) = (1-z)^{c-a-b}F(c-a,c-b,c,z). \tag{A.4}$$

Thus, the only two independent near boundary solutions are,

$$\Phi^{\mathrm{BTZ}(-)}_{\omega,k}(z,v,\phi) = e^{-i\omega v+ik\phi}z^{\Delta_-}(1+z)^{i\omega}\times F\left(\frac{1}{2}(\Delta_- - i(\omega-k)),\frac{1}{2}(\Delta_- - i(\omega+k)),\Delta_-,z^2\right), \tag{A.5}$$

$$\Phi^{\mathrm{BTZ}(+)}_{\omega,k}(z,v,\phi) = e^{-i\omega v+ik\phi}z^{\Delta_+}(1+z)^{i\omega}\times F\left(\frac{1}{2}(\Delta_+ - i(\omega+k)),\frac{1}{2}(\Delta_+ - i(\omega-k)),\Delta_+,z^2\right).$$

JHEP07(2015)041

B Thermal Green function in BTZ

The thermal Green function is obtained by taking the Fourier transform with respect to ω of the following thermal Green function in Fourier space [23],

$$G_R^{\text{thermal}}(k,\omega) = \frac{1}{2\sin(\pi\Delta_+)(\Gamma(\Delta_+))^2}\left|\Gamma\left(\frac{1}{2}(\Delta_+ + i(\omega+k))\right)\Gamma\left(\frac{1}{2}(\Delta_+ + i(\omega-k))\right)\right|^2 \times\left(\cos(\pi\Delta_+)\cosh(\pi\omega)-\cosh(\pi k)-i\sin(\pi\Delta_+)\sinh(\pi\omega)\right). \tag{B.1}$$

The Fourier transform is taken by performing integration over $\int_{-\infty}^{\infty} d\omega e^{-i\omega(v-t_1)}$ and completing the contour in the lower half ω-plane. It can be shown that the integral vanishes over the arc of sufficiently large radius. The result is a sum over the residues, which are evaluated at the poles of the gamma functions in the lower half ω-plane,

$$\begin{aligned} G_R^{\text{thermal}}(v-t_1,\omega) = {} & \frac{1}{2\sin(\pi\Delta_+)(\Gamma(\Delta_+))^2} \\ & \times\sum_n\sum_{a=\pm1}\frac{(-1)^n}{n!}e^{-i\omega_n^a(v-t_1)}\Gamma\left(\frac{1}{2}(\Delta_+ + i(\omega_n^a - ak))\right) \\ & \times\Gamma\left(\frac{1}{2}(\Delta_+ + i(\omega_n^a + ak))\right)\Gamma\left(\frac{1}{2}(\Delta_+ - i(\omega_n^a + ak))\right) \\ & \times\left[\cos(\pi\Delta_+)\cosh(\pi\omega_n^a)-\cosh(\pi k)-i\sin(\pi\Delta_+)\sinh(\pi\omega_n^a)\right]. \end{aligned} \tag{B.2}$$

These poles, $\omega(n,a)$, are the quasinormal modes of the BTZ black hole,

$$\omega_n^a = ak - i(\Delta_+ + 2n), \qquad a = \pm 1. \tag{B.3}$$

C Mixed Fourier transform of Green function in AdS

In this appendix we solve equations of the form (5.19) with the analog of the boundary conditions in (2.5) first in the frequency-momentum space. We then perform the partial Fourier transform in the frequency space. This results in the Green function in AdS which satisfies the boundary condition of (2.5). Consider (5.19), with a more general mass term,

$$z^2 p_v'' + z(-3+2i\omega z)p_v' - (-3+m^2+k^2z^2+3i\omega z)p_v = 0, \tag{C.1}$$

this equation has the following Fourier space solution, where $\nu = \sqrt{1+m^2}$,

$$p_v(k,\omega,z) = e^{-i\omega z}z^2\left(A(\omega)J_\nu\left(z\sqrt{\omega^2-k^2}\right)+B(\omega)J_{-\nu}\left(z\sqrt{\omega^2-k^2}\right)\right). \tag{C.2}$$

Using the property of the Bessel function for small argument, the following near boundary behaviour of the solution is obtained,

$$p_v(k,\omega,z)\xrightarrow{z\to0} z^2\left(A(\omega)\left(\frac{z\sqrt{\omega^2-k^2}}{2}\right)^\nu\frac{1}{\Gamma(1+\nu)}+B(\omega)\left(\frac{z\sqrt{\omega^2-k^2}}{2}\right)^{-\nu}\frac{1}{\Gamma(1-\nu)}\right). \tag{C.3}$$

JHEP07(2015)041

The delta function boundary condition in (2.5) in the time domain requires that near the boundary the wave function in Fourier space solution goes to

$$p_v(k,\omega,z) \xrightarrow{z\to 0} \frac{1}{2\pi}\cdot z^{\Delta_-}. \tag{C.4}$$

This determines $B(\omega)$ to be

$$B(\omega) = \frac{\Gamma(1-\nu)}{2\pi}\left(\frac{\sqrt{\omega^2-k^2}}{2}\right)^{\nu}, \tag{C.5}$$

where, $\Delta_\pm = 2 \pm \nu$.

We now use the following asymptotic behaviour of Bessel functions to obtain the behaviour of the solution near the origin of AdS,

$$\begin{aligned} J_\nu(x) &\xrightarrow{x\to\infty} \sqrt{\frac{2}{\pi x}}\cos\left(x-\frac{\nu\pi}{2}-\frac{\pi}{4}\right), \\ J_{-\nu}(x) &\xrightarrow{x\to\infty} \sqrt{\frac{2}{\pi x}}\left[\cos(\pi\nu)\cos\left(x-\frac{\nu\pi}{2}-\frac{\pi}{4}\right)-\sin(\pi\nu)\sin\left(x-\frac{\nu\pi}{2}-\frac{\pi}{4}\right)\right]. \end{aligned} \tag{C.6}$$

As $z\to\infty$, the solution,

$$\begin{aligned} p_v(k,\omega,z) \longrightarrow e^{-i\omega z}z^2\sqrt{\frac{2}{\pi z}}(\omega^2-k^2)^{-\frac{1}{4}}\Big[&(A(\omega)+B(\omega)\cos(\pi\nu))\cos\left(x-\frac{\nu\pi}{2}-\frac{\pi}{4}\right) \\ &-B(\omega)\sin(\pi\nu)\sin\left(x-\frac{\pi\nu}{2}-\frac{\pi}{4}\right)\Big], \end{aligned} \tag{C.7}$$

where, $x = z\sqrt{\omega^2-k^2}$. The solution near the origin has both ingoing and outgoing behaviour due to the presence of cosine and sine. In order to impose ingoing boundary condition at origin, the solution is rewritten as a linear combination of ingoing and outgoing solutions,

$$p_v(k,\omega,z) = C(\omega)e^{-i(x-\frac{\nu\pi}{2}-\frac{\pi}{4})} + D(\omega)e^{i(x-\frac{\nu\pi}{2}-\frac{\pi}{4})}, \tag{C.8}$$

where C and D in terms of A and B, are

$$C(\omega) = \frac{1}{2}\left(A(\omega)+B(\omega)e^{-i\pi\nu}\right), \tag{C.9}$$

$$D(\omega) = \frac{1}{2}\left(A(\omega)+B(\omega)e^{i\pi\nu}\right). \tag{C.10}$$

The ingoing boundary condition at origin, means that $D(\omega)=0$, hence,

$$A(\omega) = -B(\omega)e^{i\pi\nu}. \tag{C.11}$$

Substituting this in (C.2), we obtain,

$$\begin{aligned} p_v(k,\omega,z) &= B(\omega)e^{-i\omega z}z^2\left[-e^{i\pi\nu}J_\nu(x)+J_{-\nu}(x)\right] \\ &= -i\sin(\pi\nu)e^{i\pi\nu}B(\omega)e^{-i\omega z}zH^{(2)}_{-\nu}(x). \end{aligned} \tag{C.12}$$

JHEP07(2015)041

The Fourier transform of the above equation with respect to ω, gives

$$G_F^{\rm AdS}(v,k,z) = -ie^{i\pi\nu}\frac{1}{2\Gamma(\nu)}z^2\int_{-\infty}^{\infty}d\omega\, e^{-i\omega(v+z)}\left(\frac{\sqrt{\omega^2-k^2}}{2}\right)^{\nu}H^{(2)}_{-\nu}\left(z\sqrt{\omega^2-k^2}\right), \quad \text{(C.13)}$$

using the integral representation of $H^{(2)}_{-\nu}(x)$,

$$H^{(2)}_{-\nu}(x) = \frac{i}{\pi}e^{-\frac{i\pi\nu}{2}}x^{-\nu}\int_0^{\infty}dy\,\exp\left[-\frac{i}{2}\left(y+\frac{x^2}{y}\right)\right]y^{\nu-1}, \quad \text{(C.14)}$$

$$\begin{aligned} G_F^{\rm AdS}(v,k,z) &= \frac{e^{\frac{i\pi\nu}{2}}}{2^{\nu}2\pi\Gamma(\nu)}z^{2-\nu}\int_0^{\infty}dy\,y^{\nu-1}\exp\left[-\frac{i}{2}\left(y-\frac{z^2k^2}{y}\right)\right] \quad \text{(C.15)}\\ &\quad\times\int_{-\infty}^{\infty}d\omega\,\exp\left[-i\left(\frac{\omega^2z^2}{2y}+\omega(v+z)\right)\right]\\ &= \frac{e^{-i\frac{\pi}{4}}e^{\frac{i\pi\nu}{2}}}{2^{\nu}2\pi\Gamma(\nu)}\sqrt{2\pi}z^{1-\nu}\int_0^{\infty}dy\,y^{\nu-\frac{1}{2}}\exp\left[\frac{i}{2}\left(y\left(\frac{2v}{z}+\left(\frac{v}{z}\right)^2\right)+\frac{z^2k^2}{y}\right)\right]\\ &= \frac{e^{-i\frac{\pi}{4}}e^{\frac{i\pi\nu}{2}}}{2^{\nu}2\pi\Gamma(\nu)}\sqrt{2\pi}z^{1-\nu}2\left(\frac{kz^2}{\sqrt{v^2+2vz}}\right)^{\nu+\frac{1}{2}}K_{-\nu-\frac{1}{2}}\left(-ik\sqrt{v^2+2vz}\right)\\ &= \frac{1}{2^{\nu}\Gamma(\nu)}\frac{\sqrt{2\pi}}{2}z^{2+\nu}\left(\frac{k}{\sqrt{v^2+2vz}}\right)^{\nu+\frac{1}{2}}H^{(1)}_{-\nu-\frac{1}{2}}\left(k\sqrt{v^2+2vz}\right). \end{aligned}$$

In the last step, $K_\lambda(x) = \frac{i\pi}{2}e^{\frac{i\pi\lambda}{2}}H^{(1)}_\lambda(ix)$, has been used. The retarded two point function is obtained from the Feynman two point function using the relation

$$G_R(t,t') = \theta(t-t')\left(G_F(t,t')+G_F^*(t,t')\right). \quad \text{(C.16)}$$

The following properties of the Bessel functions,

$$\begin{aligned} H^{(1)}_\lambda(x)^* &= H^{(2)}_\lambda(x), \quad \text{(C.17)}\\ H^{(1)}_\lambda + H^{(2)}_\lambda &= i\csc(\pi\lambda)(e^{-i\pi\lambda}-e^{i\pi\lambda})J_\lambda(x), \end{aligned}$$

are used in last two equations, to obtain the retarded Green function which is given by

$$\begin{aligned} G_R^{\rm AdS}(v-t_1,k,z) &= C\theta(v-t_1)z^{2+\nu}\left(\frac{k}{\sqrt{(v-t_1)^2+2(v-t_1)z}}\right)^{\nu+\frac{1}{2}} \quad \text{(C.18)}\\ &\quad\times J_{-\nu-\frac{1}{2}}\left(k\sqrt{(v-t_1)^2+2(v-t_1)z}\right), \end{aligned}$$

where, $C = \frac{2^{\frac{1}{2}-\nu}\sqrt{\pi}}{\Gamma(\nu)}$. Though we started out by assuming ν is not an integer and the two independent solutions are given by (C.2), the discussion can be generalized to the case when ν is an integer, leading to the same final result given in (C.18). A simple way to see this is that in the final result the order of the Bessel function is fractional.

JHEP07(2015)041

D Recursion relation for retarded Green functions in AdS

In this appendix for completeness we obtain the recursion relation for the mixed Fourier space retarded Green function in AdS_{d+1} at $v = 0$. This is useful to implement the recursive algorithim to obtain the thermalizing Green function in thin shell Vaidya geometries. The solution for a scalar field in mixed Fourier space in AdS_{d+1}, has the following dependence on the Bessel function,

$$\Phi^{\rm AdS}(v=0,k,z;t_1) = z^{\Delta_+} R(z). \tag{D.1}$$

Here we have assumed $t_1 < 0$.

$$R(z) = C\left(\frac{k}{\sqrt{t_1^2 - 2t_1 z}}\right)^{\nu+\frac{1}{2}} J_{-\nu-\frac{1}{2}}\left(k\sqrt{t_1^2 - 2t_1 z}\right), \tag{D.2}$$

where, from (3.3) and (C.18), we see that, $\Delta_+ = d/2+\nu$. The differential equation satisfied by $R(z)$ is,

$$(t_1 - 2z)R''(z) + 2(\lambda - 1)R'(z) + k^2 t_1 R(z) = 0. \tag{D.3}$$

Substituting the ansatz, $R(z) = \sum_{n=0}^{\infty} \tilde{J}_n z^n$ in the above equation, the following recursion relation for $\tilde{J}_n$ is obtained,

$$\tilde{J}_n = \frac{2(n-1)(n-1-\lambda)\tilde{J}_{n-1} - k^2 t_1 \tilde{J}_{n-2}}{t_1 n(n-1)}; \qquad \text{for } n \geq 2. \tag{D.4}$$

To get the solution of (D.2) from the above recursion relation, $\tilde{J}_0$ and $\tilde{J}_1$ are chosen to be,

$$\tilde{J}_0 = C\left(\frac{k}{|t_1|}\right)^{\nu+\frac{1}{2}} J_{-\nu-\frac{1}{2}}(|k||t_1|), \tag{D.5}$$

$$\tilde{J}_1 = C\left(\frac{k}{|t_1|}\right)^{\nu+\frac{1}{2}} k\, J_{-\nu-\frac{3}{2}}(|k||t_1|). \tag{D.6}$$

Thus we obtain the Frobenius series expansion of AdS scalar field solution, around $z = 0$,

$$\Phi^{\rm AdS}(v=0,k,z;t_1) = z^{\Delta_+} \sum_{n=0}^{\infty} \tilde{J}_n z^n. \tag{D.7}$$

References

[1] B.V. Jacak and B. Müller, *The exploration of hot nuclear matter*, *Science* **337** (2012) 310 [INSPIRE].

[2] M. Greiner, O. Mandel, T.W. Hänsch and I. Bloch, *Collapse and revival of the matter wave field of a Bose-Einstein condensate*, *Nature* **419** (2002) 51 [cond-mat/0207196].

[3] A. Widera, F. Gerbier, S. Fölling, T. Gericke, O. Mandel and I. Bloch, *Coherent collisional spin dynamics in optical lattices*, *Phys. Rev. Lett.* **95** (2005) 190405 [cond-mat/0505492].

[4] L.E. Sadler, J.M. Higbie, S.R. Leslie, M. Vengalattore and D.M. Stamper-Kurn, *Spontaneous symmetry breaking in a quenched ferromagnetic spinor Bose-Einstein condensate*, *Nature* **443** (2006) 312 [cond-mat/0605351].

JHEP07(2015)041

[5] T. Kinoshita, T. Wenger and D.S. Weiss, *A quantum Newton's cradle*, *Nature* **440** (2006) 900.

[6] S. Kalyana Rama and B. Sathiapalan, *On the role of chaos in the AdS/CFT connection*, *Mod. Phys. Lett.* **A 14** (1999) 2635 [hep-th/9905219] [INSPIRE].

[7] U.H. Danielsson, E. Keski-Vakkuri and M. Kruczenski, *Spherically collapsing matter in AdS, holography and shellons*, *Nucl. Phys.* **B 563** (1999) 279 [hep-th/9905227] [INSPIRE].

[8] S.B. Giddings and S.F. Ross, *D3-brane shells to black branes on the Coulomb branch*, *Phys. Rev.* **D 61** (2000) 024036 [hep-th/9907204] [INSPIRE].

[9] U.H. Danielsson, E. Keski-Vakkuri and M. Kruczenski, *Black hole formation in AdS and thermalization on the boundary*, *JHEP* **02** (2000) 039 [hep-th/9912209] [INSPIRE].

[10] S.B. Giddings and A. Nudelman, *Gravitational collapse and its boundary description in AdS*, *JHEP* **02** (2002) 003 [hep-th/0112099] [INSPIRE].

[11] S. Lin and E. Shuryak, *Toward the AdS/CFT Gravity Dual for High Energy Collisions. 3. Gravitationally Collapsing Shell and Quasiequilibrium*, *Phys. Rev.* **D 78** (2008) 125018 [arXiv:0808.0910] [INSPIRE].

[12] P.M. Chesler and L.G. Yaffe, *Horizon formation and far-from-equilibrium isotropization in supersymmetric Yang-Mills plasma*, *Phys. Rev. Lett.* **102** (2009) 211601 [arXiv:0812.2053] [INSPIRE].

[13] S. Bhattacharyya and S. Minwalla, *Weak Field Black Hole Formation in Asymptotically AdS Spacetimes*, *JHEP* **09** (2009) 034 [arXiv:0904.0464] [INSPIRE].

[14] P.M. Chesler and L.G. Yaffe, *Boost invariant flow, black hole formation and far-from-equilibrium dynamics in $N = 4$ supersymmetric Yang-Mills theory*, *Phys. Rev.* **D 82** (2010) 026006 [arXiv:0906.4426] [INSPIRE].

[15] G. Beuf, M.P. Heller, R.A. Janik and R. Peschanski, *Boost-invariant early time dynamics from AdS/CFT*, *JHEP* **10** (2009) 043 [arXiv:0906.4423] [INSPIRE].

[16] M.P. Heller, R.A. Janik and P. Witaszczyk, *The characteristics of thermalization of boost-invariant plasma from holography*, *Phys. Rev. Lett.* **108** (2012) 201602 [arXiv:1103.3452] [INSPIRE].

[17] M.P. Heller, R.A. Janik and P. Witaszczyk, *A numerical relativity approach to the initial value problem in asymptotically Anti-de Sitter spacetime for plasma thermalization — an ADM formulation*, *Phys. Rev.* **D 85** (2012) 126002 [arXiv:1203.0755] [INSPIRE].

[18] J. Abajo-Arrastia, J. Aparicio and E. Lopez, *Holographic Evolution of Entanglement Entropy*, *JHEP* **11** (2010) 149 [arXiv:1006.4090] [INSPIRE].

[19] T. Albash and C.V. Johnson, *Evolution of Holographic Entanglement Entropy after Thermal and Electromagnetic Quenches*, *New J. Phys.* **13** (2011) 045017 [arXiv:1008.3027] [INSPIRE].

[20] H. Ebrahim and M. Headrick, *Instantaneous Thermalization in Holographic Plasmas*, arXiv:1010.5443 [INSPIRE].

[21] V. Balasubramanian et al., *Holographic Thermalization*, *Phys. Rev.* **D 84** (2011) 026010 [arXiv:1103.2683] [INSPIRE].

[22] J. Aparicio and E. Lopez, *Evolution of Two-Point Functions from Holography*, *JHEP* **12** (2011) 082 [arXiv:1109.3571] [INSPIRE].

JHEP07(2015)041

[23] V. Balasubramanian et al., *Thermalization of the spectral function in strongly coupled two dimensional conformal field theories*, *JHEP* **04** (2013) 069 [arXiv:1212.6066] [INSPIRE].

[24] N. Callebaut et al., *Holographic Quenches and Fermionic Spectral Functions*, *JHEP* **10** (2014) 172 [arXiv:1407.5975] [INSPIRE].

[25] V.E. Hubeny, M. Rangamani and T. Takayanagi, *A covariant holographic entanglement entropy proposal*, *JHEP* **07** (2007) 062 [arXiv:0705.0016] [INSPIRE].

[26] V. Keranen and P. Kleinert, *Non-equilibrium scalar two point functions in AdS/CFT*, *JHEP* **04** (2015) 119 [arXiv:1412.2806] [INSPIRE].

[27] A. Núñez and A.O. Starinets, *AdS/CFT correspondence, quasinormal modes and thermal correlators in $N = 4$ SYM*, *Phys. Rev.* **D 67** (2003) 124013 [hep-th/0302026] [INSPIRE].

[28] G. Policastro, D.T. Son and A.O. Starinets, *From AdS/CFT correspondence to hydrodynamics*, *JHEP* **09** (2002) 043 [hep-th/0205052] [INSPIRE].

[29] D.T. Son and A.O. Starinets, *Minkowski space correlators in AdS/CFT correspondence: Recipe and applications*, *JHEP* **09** (2002) 042 [hep-th/0205051] [INSPIRE].

[30] A. Buchel and J.T. Liu, *Thermodynamics of the $N = 2^*$ flow*, *JHEP* **11** (2003) 031 [hep-th/0305064] [INSPIRE].

[31] D. Birmingham, *Choptuik scaling and quasinormal modes in the AdS/CFT correspondence*, *Phys. Rev.* **D 64** (2001) 064024 [hep-th/0101194] [INSPIRE].

[32] D. Birmingham, I. Sachs and S.N. Solodukhin, *Conformal field theory interpretation of black hole quasinormal modes*, *Phys. Rev. Lett.* **88** (2002) 151301 [hep-th/0112055] [INSPIRE].

[33] P.K. Kovtun and A.O. Starinets, *Quasinormal modes and holography*, *Phys. Rev.* **D 72** (2005) 086009 [hep-th/0506184] [INSPIRE].

[34] G.T. Horowitz and V.E. Hubeny, *Quasinormal modes of AdS black holes and the approach to thermal equilibrium*, *Phys. Rev.* **D 62** (2000) 024027 [hep-th/9909056] [INSPIRE].

[35] S.A. Stricker, *Holographic thermalization in $N = 4$ Super Yang-Mills theory at finite coupling*, *Eur. Phys. J.* **C 74** (2014) 2727 [arXiv:1307.2736] [INSPIRE].

[36] S. Banerjee, R. Iyer and A. Mukhopadhyay, *The holographic spectral function in non-equilibrium states*, *Phys. Rev.* **D 85** (2012) 106009 [arXiv:1202.1521] [INSPIRE].

[37] A. Mukhopadhyay, *Nonequilibrium fluctuation-dissipation relation from holography*, *Phys. Rev.* **D 87** (2013) 066004 [arXiv:1206.3311] [INSPIRE].

[38] S. Datta and J.R. David, *Higher Spin Quasinormal Modes and One-Loop Determinants in the BTZ black Hole*, *JHEP* **03** (2012) 079 [arXiv:1112.4619] [INSPIRE].

[39] S. Datta and J.R. David, *Higher spin fermions in the BTZ black hole*, *JHEP* **07** (2012) 079 [arXiv:1202.5831] [INSPIRE].

[40] P. Calabrese and J.L. Cardy, *Time-dependence of correlation functions following a quantum quench*, *Phys. Rev. Lett.* **96** (2006) 136801 [cond-mat/0601225] [INSPIRE].

JHEP07(2015)041